Lateral Torsional Buckling of Tapered Beam

Author: Jovana Lukac

Supervisor: Ing. Michal Jandera Ph.D.

University: Czech Technical University in Prague

University: Czech Technical University in Prague

Date: 20.12.2013

Declaration on word of honour

I declare that submitted project was written by me and I have stated all information resources used in conformity with the Methodical guide for ethical development of university final thesis.

Abstract

Tapered steel members are commonly used over prismatic members because of their structural efficiency: by optimizing cross section utilization, significant material can be saved. However, if proper rules and guidance are not developed for these types of members, safety verification will lead to an over prediction of the material to be used. In this paper, the case of beam with linear varying web is studied. It is the purpose of this paper to: (i) review recent proposals for the stability verification of this type of beam; (ii) carry out FEM numerical simulations covering several combinations of bending moment about strong axis, M_y, and levels of taper; (iii) compare results to a) existing rules in EC3-1-1 (General Method); b) application of the design procedure proposed by Marques et al; c) Merchant-Rankine procedure for stability verification of tapered beams.

Keywords

Stability verification, Eurocode 3, Non-uniform members, Tapered beams, Finite element analysis, Steel structures

1 Introduction

This work is mainly based on the verification of the existing methods for the checking of the stability of members loaded mainly with bending moments at room temperature as well as elevated temperature. It concerns the elastic lateral torsional buckling of linearly web tapered I-beams with double-symmetric cross-sections, under linear bending moment distributions.

Web tapered beams are quite usual members in steel construction nowadays. Their use is largely widespread since they allow significant material saving and much consistent design which leads to optimization of the structure. For the case of uniform bending moment distribution, it is clear that prismatic member would be the best option because in that case all cross-sections would be fully utilized (considering first order forces). Tapered members are usually adopted in order to optimize the load capacity at each cross-section according to the respective distribution of stresses.

Though beams in the constructions, and mainly as members in portal frames, are generally loaded in bending and compression at the same time, it is clear that the problem of bending is the most difficult one in the context of lateral torsional buckling.

EC3 provides several methods for the stability verification of members and frames. The stability of prismatic members under bending in EC3-1-1 [5] is checked by application of clause 6.3.2 – stability of beams. Regarding the stability of a tapered beam, clause 6.3.2 does not apply.

It should be said that one of additional problems that occur when dealing with tapered beams is that they are usually made of class 4 sections in order to optimize the member. This fact will also be studied in this work.

2 State of the art

Lateral-torsional buckling is an instability phenomenon characterized by the occurrence of large transversal displacements and rotation about the member axis, under bending moment about the major axis (y axis). This instability phenomenon involves lateral bending (about z axis) and torsion of cross section.
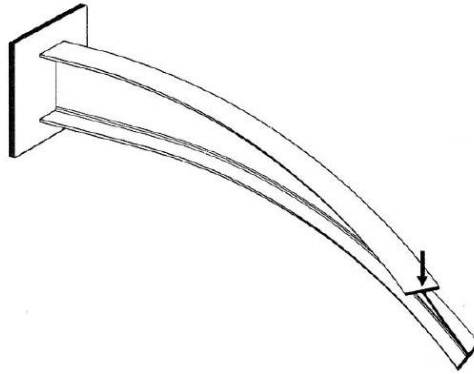

Figure 2-1 Example of lateral-torsional buckling phenomenon

The part of the section that is compressed (compressed flange in case of I section) undergoes lateral deformation. This part is considered to be continuously restrained by the part of the section that is in tension, which initially does not have any tendency to move laterally.

A fundamental role on the analysis of this type of phenomena plays elastic critical moment (M_{cr}), which is the maximum value of bending moment supported by a beam without imperfections. There are many proposals on evaluating the elastic critical moment and some of them are presented below.

2.1 General method

As it has been mentioned already, Eurocode 3, part 1, provides several methods for the stability verification of prismatic members but none of the methods is applicable for stability of tapered beams. The code is referring to the clause 6.3.4 for determination of buckling resistance of such a member (General method). According to this method, overall resistance to out-of-plane buckling for any structural component can be verified by ensuring that:

$$\frac{\chi_{op} \cdot \alpha_{ult,k}}{\gamma_{M1}} \geq 1.0 \qquad\qquad 2.1$$

where

$\alpha_{ult,k}$ is the minimum load amplifier of the design loads to reach the characteristic resistance of the most critical cross section of the structural component considering its in-plane behaviour without taking lateral or lateral-torsional buckling into account, but however accounting for all effects due to in plane geometrical deformation and imperfections, global and local, where relevant;

χ_{op} is the reduction factor for the non-dimensional slenderness $\overline{\lambda}_{op}$, to take account lateral and lateral torsional buckling;

γ_{M1} is the partial safety coefficient for instability effects (in most National Annexes is adopted as 1,0).

Global non-dimensional slenderness $\overline{\lambda}_{op}$ for the structural component should be determined from:

$$\overline{\lambda}_{op} = \sqrt{\frac{\alpha_{ul.k}}{\alpha_{cr,op}}} \qquad 2.2$$

where

$\alpha_{cr,op}$ is the minimum amplifier for the in-plane design loads to reach the elastic critical resistance of the structural component with regards to lateral or lateral-torsional buckling without accounting for in-plane flexural buckling.

The reduction factor χ_{op} may be determined from either of the following methods:

a) the minimum value of
-   χ_z for lateral buckling according to 6.3.1 of [5]
-   χ_{op} for lateral-torsional buckling according to 6.3.2 of [5],

each calculated for the global non-dimensional slenderness $\overline{\lambda}_{op}$.
This leads to:

$$\frac{N_{Ed}}{N_{Rk}/\gamma_{M1}} + \frac{M_{y,Ed}}{M_{y,Rk}/\gamma_{M1}} \leq \chi_{op} \qquad 2.3$$

b) a value interpolated between the values χ_z and χ_{LT} as determined in a) by using the formula for $\alpha_{ult,k}$ corresponding to the critical cross section.
This leads to:

$$\frac{N_{Ed}}{\chi_z \cdot N_{Rk}/\gamma_{M1}} + \frac{M_{y,Ed}}{\chi_{LT} \cdot M_{y,Rk}/\gamma_{M1}} \leq 1 \qquad 2.4$$

In order to determine $\alpha_{cr,op}$ and $\alpha_{ul.k}$ the code is not giving any consistent procedure but suggesting use of FEA software which is not practical solution.
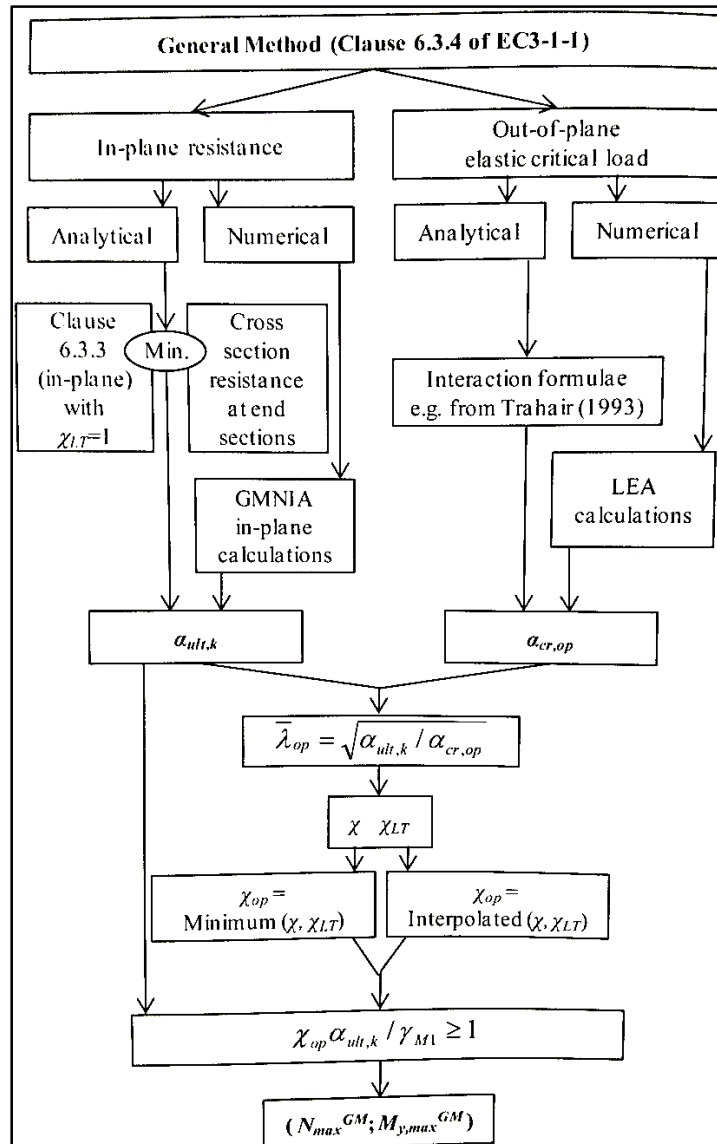
Figure 2-2 The flow chart for the application of the General Method, see [8]

There have been done many research on the buckling resistance of the web-tapered beam that were based on this method.

Kitipornchai and Trahair [5] give an analytical solution for elastic critical moment of tapered beam, covering any type of tapered I-beam and loading.

Expressions for the elastic critical moment are given also by Galéa (1986) [4] in which the elastic critical load of a web-tapered beam subjected to uniform bending moment distribution is obtained by the determination of an equivalent height and moments of inertia. The elastic critical moment of beams subjected to uniform bending moment and fork supports can be obtained using the expressions for the prismatic beams as long as the equivalent geometrical properties are used, given by:

$$h_{eq} = h_{max} \sqrt{0.283 + 0.434\gamma + 0.283\gamma^2} \qquad 2.5$$

where

h_{max} is the maximum depth of the member and

$\gamma(= h_{min} / h_{max})$ is the taper ratio, and

$$I_{z,eq} = I_z ,$$

<div align="right">2.6</div>

$$I_{T,eq} = \frac{I_{T,max} + I_{T,min}}{2} .$$

<div align="right">2.7</div>

In case of non-uniform bending moment distribution, there are some coefficients provided to account for this effects. Also, for fully-restrained rotation about the weak axis of the cross-section at the end of the member, the formulae for the equivalent beam depth slightly changes, but all this can be found in [4].

Boissonnade N. and Braham M. (2002) gave the expressions for the elastic critical moment [2] in which is considered monosymmetric cross-section with linear distribution of bending moments and made a Mathcad file (ELTBTB2) for calculating the same.

According to the most recent studies of Marques L. et al. (2012) [3], the second order theory formulae for lateral-torsional buckling of beams with a linearly tapered web symmetrical to its centroid are derived using first yield criterion to find the resistance of the tapered beam at the most stressed cross-section. This proposal gives a stable level of accuracy and certainty regarding its application that so far the general method in EC3-1-1 was not able to provide. The whole procedure is presented in *Design procedures* chapter.

2.2 Comparison of the available software for the calculation of the critical load multiplier

2.2.1 ELTBTB2

This programme is actually a Mathcad programme, made by Marc Braham, for determination of the critical load multiplier for lateral torsional buckling of web-tapered beams. The programme is based on differential equation for the equilibrium of a monosymmetric beam.

- The programme is easy to use;
- Allows for the linear distribution of moments (no axial compression can be taken into account);
- No intermediate load can be taken into account;
- It is solving the problem for the beams on two supports, with no lateral restrains.

2.2.2 Alpha_Cr

Alpha_Cr is a programme for the determination of critical loads, on basis of the Finite Element Method (FEM). Some characteristics of the programme are:

- The program assumes mono-symmetric cross sections;
- Local buckling of the cross sections (Class 4 sections) is not considered;
- The loads can be applied in the xz-plane;
- Critical load factors for the general stability problem of lateral torsional buckling and the special cases of flexural buckling and torsional buckling can be calculated;

2.2.3 LTBeamN

LTBeamN is the software for determination of elastic stability (in-plane as well as out-of-plane) of straight beams deflected and/or compressed by determining in particular critical load factor μ_{cr}. Advantages of using this software are:

- The longitudinal profile of a beam can be non-uniform (without discontinuities), with the linear dimensional changes on all or part of their length. The distribution of applied loads (M and N), the support conditions in the plan and the conditions for maintaining out-of-plan can be very varied;
- Gives information on the shape of the fundamental mode of elastic instability (first eigenmode), as well as higher order modes own if required;
- An indication of the critical load for the in-plane buckling is also provided.

Modelling the behaviour of the beam uses a technique of finite element "bar" type that requires a discretization of the beam into a number of small. The degrees of freedom taken into account at each node are four, including:

- ✓ lateral displacement (v)
- ✓ longitudinal rotation - twist (q)
- ✓ rotation lateral bending (v')
- ✓ warping deformation (q') ;
- Besides the double-symmetric and mono-symmetric sections, it covers any profiles defined by the geometric properties;

2.3 Members with intermediate restrains

It is very common situation to have partial bracings that only prevent transvers displacements of the tension flange. These partial bracings are really effective in increasing the resistance to out-of-plane buckling.

The elastic critical moment for lateral-torsional buckling, $M_{cr,0}$, for an uniform moment and standard bracing conditions at each end of the segment (no transverse displacement, no rotation around the longitudinal axis and free rotation in plane) is given by:

$$M_{cr0} = (\frac{i_s^2}{2a})N_{cr} ,$$ 2.8

where

N_{crT} is the elastic critical load in a torsional mode, given by:

$$N_{crT} = \frac{1}{i_s^2}(\frac{\pi^2 EI_z a^2}{L_t^2} + \frac{\pi^2 EI_w}{L_t^2} + GI_t) .$$ 2.9

Here $M_{cr,0}$ should be calculated using the properties of the smallest cross section.

For mono-symmetric cross sections with uniform flanges, the elastic critical moment for an arbitrary bending moment diagram is given by:

$$M_{cr} = (\frac{1}{m_t c_0^2})M_{cr0} ,$$ 2.10

where

m_t is the equivalent uniform moment factor, or in case of linear moment distribution, it depends on the ratio between the smaller and the larger bending moment, β_t (sagging moment is positive). This coefficient β_t can be found in [8]. When the variation of the bending moment is not linear, special expressions are also provided in [8], chapter 4.3.3;

c_0 is the equivalent cross section factor given in the Table 4.7 in [8]

2.4 Stable length of a segment of a member

It should be said that, apart from the General method, Eurocode gives rules for defining the stable lengths of segment containing plastic hinges for out-of-plane buckling, covering haunches which can be sort of tapered members. Clause (1)B of BB.3.2 in EN 1993-1-1 specifies the length of the segment of a member between the restrained section at a plastic hinge location and the adjacent lateral restraint in which lateral torsional buckling effects may be ignored. This length is given as:

European Erasmus Mundus Master
Sustainable Constructions under natural hazards and catastrophic events
520121-1-2011-1-CZ-ERA MUNDUS-EMMC

ruscos

$$L_m = 0,85 \frac{38 \cdot i_z}{\sqrt{\frac{1}{57,4}\left(\frac{N_{Ed}}{A}\right) + \frac{1}{756 C_1^2}\left(\frac{W_{pl,y}^2}{A \cdot I_t}\right)\left(\frac{f_y}{235}\right)^2}} \qquad 2.11$$

where

N_{Ed} is the design value of the compression force in the member

$\dfrac{W_{pl,y}^2}{A \cdot I_t}$ is the maximum value in the segment

A is the cross sectional area [mm²] at the location where $\dfrac{W_{pl,y}^2}{A \cdot I_t}$ is a maximum of the

     tapered member

$W_{pl,y}$ is the plastic section modulus of the member

I_t is the torsional constant of the member

f_y is the yield strength in [N/mm²]

i_z is the minimum value of the radius of gyration in the segment, provided that the member is restrained at the hinge as required by 6.3.5 and that the other end of segment is restrained either by a lateral restraint to the compression flange where one flange is in compression throughout the length of the segment, or by a torsional restraint, or by a lateral restraint at the end of the segment and a torsional restraint to the member at a distance that satisfies the requirements for L_s.

$$L_s = 0.85 \frac{\sqrt{C_n} L_k}{c} \qquad 2.12$$

where

L_k is the length derived for a uniform member with a cross-section equal to the shallowest section

C_n see BB.3.3.2

c is the taper factor for a non-uniform member with constant flanges, for which $h \geq 1.2b$ and $h/t_f \geq 20$ the taper factor c should be obtained as follows:

$$c = 1 + \frac{3}{\left(\dfrac{h}{t_f} - 9\right)}\left(\frac{h_{max}}{h_{min}} - 1\right)^{2/3} \qquad 2.13$$

Still, this method is not saying how to evaluate the resistance of the tapered member but determining the stable length of the segment of the member.

2.5   Choice of a proper taper ratio

Since it is not clear that a higher taper ratio will lead to a higher (relative) resistance it was investigated in [2] and the quantification of the "unused" resistance in a tapered beam with a bending moment distribution ψ (ratio between the smaller and bigger bending moments at the two ends of the beam) is presented below.
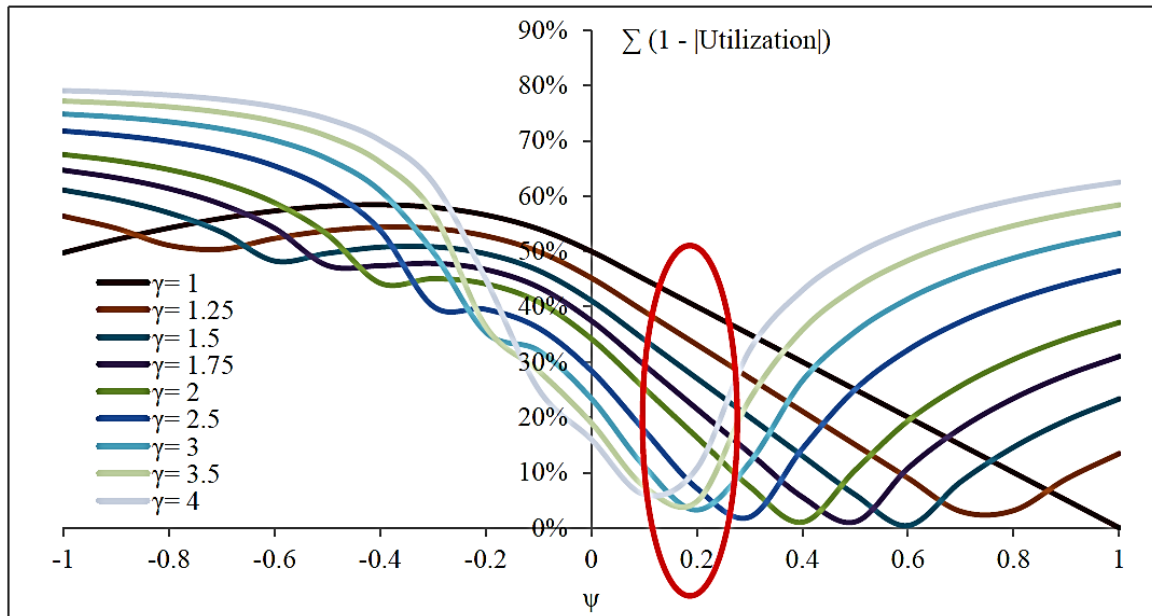

Figure 2-3 Quantification of the "unused" resistance [2]

Using the graph presented above, the best taper ratio for a given bending moment distribution can be identified in a really practical way.

2.6   Choice of an appropriate buckling curve

Due to the varying height of the member, more than one buckling curve may exist for a tapered member (e.g. in which the ratio *h/b≤2* and *h/b>2* (height/width) is present in the same tapered beam or beam-column). As an alternative and on the safe side, the buckling curve corresponding to the highest imperfection factor can be chosen, leading to conservative levels of resistance.

The existing buckling curves are adopted to best fit the numerical results for uniform members with a sinusoidal imperfection. Therefore, they should not be applicable for the members with non-uniform height.

It was demonstrated in [6] that use of flexural buckling curves in the General method can lead to over safe results (more than 30% relatively to full non-linear numerical analysis). On the other hand, if the lateral torsional buckling curves for rolled sections or equivalent welded sections (clause 6.3.2.3 of EC3-1-1) are considered, results can reach differences of 30% on the unsafe side. Also in [3] is shown that the consideration of the buckling curves *a, b, c* or *d* is not adequate for application of the General Method and, as a result, proper modifications are proposed (introduction of the "over-strength" factor). This is illustrated in section *2.8 Design procedure* of this document.

2.7 Cross-section class and the location of the critical cross-section

The first order failure location of tapered beam-columns varies with varying levels of axial force relatively to the applied bending moment leading. With the increase of the axial force the maximum utilization location, $x_{c,MN}^{I}$, moves towards the smallest cross section, which is the first order failure location of the <u>column</u>, $x_{c,N}^{I}$ as the axial force is constant.

An iterative procedure should be carried out in order to define the class of the cross-section of a tapered member. This would require evaluation of the stresses (1st and 2nd order) along the member. How this is not practical approach, it is suggested to adopt highest class which may result in over-conservative design as the cross-section class may be higher in an interval of the member which is not critical in terms of utilization. Also, instead of defining the critical design location, equivalent cross-section property formulae for the calculation of elastic critical forces should be used.

With the increase of tapering, both the resistance and the plateau length are increasing (this increase is less significant for the higher taper ratios, which can be seen in the figures 2-4 presented below and derived in Marques et al. (2013), see [2]). This influence of tapering is taken into account by introducing the coefficient $x_{c,N}^{I}$ which is defined in [2]. Since the location of the critical cross-section will have to change due to the asymmetry of either the 1st or 2nd order utilization ratios this factor $\beta\left(x_{c}^{II}\right)$ accounts for this effect.

In case of prismatic members, the second order failure location is coincident with the first order failure location, leading to the same load amplifier for both cases, $\alpha_{ult,k}(L/2) = M_{y,Rk}(L/2) / M_{y,Ed}(L/2)$. For this case, the increase in resistance of the parabolic bending moment case relatively to the uniform bending moment case is due to smaller size of the plastic zone that surrounds the failure location and as a result, due to a higher "supporting" action from the unyielded areas. Differently saying, the "over-strength" factor is an intuitive parameter proposed in [2] to qualitatively describe not only the lower spread of plasticity around the failure location, but also the increase in resistance for a given beam with $\gamma_{h} \neq 1$ and $\psi \neq 1$ relatively to the reference case of $\gamma_{h} = \psi = 1$.

The utilization ratio may be determined from:

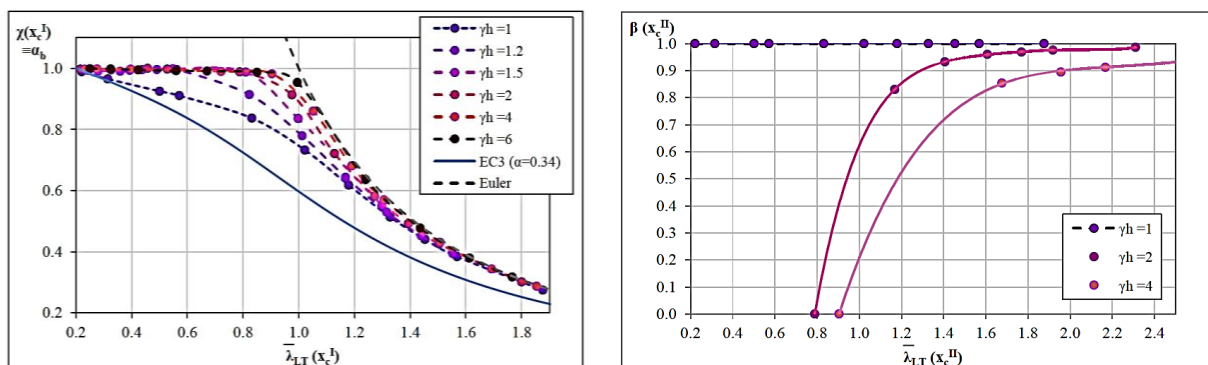$$\varepsilon(x) = \frac{M_{y,Ed}(x)}{M_{pl,y,Rd}(x)} \leq 1.0 \,. \qquad 2.14$$

Figure 2-4 Buckling curve and Imperfection factors for tapered beams [2]

This coefficient $\beta\left(x_c^{II}\right)$ can also be found as φ ("over-strength" factor). If the factor φ is determined, the verification is always based on $x_c^{I} \cdot \varphi$. This leads to:

$$\overline{\lambda}(x_c^{II}) = \sqrt{\frac{\alpha_{ult,k}(x_c^{II})}{\alpha_{cr}}} = \sqrt{\frac{\varphi \cdot \alpha_{ult,k}(x_c^{I})}{\alpha_{cr}}} = \overline{\lambda}(x_c^{I})\sqrt{\varphi}.$$

2.15

As for the cross section verification, it should be performed in a sufficient number of locations in order to find the cross section with the highest first order utilization.

In addition to this, in case of **elevated temperatures** the class section can be classified as for normal temperature design with a reduced value for ε as given in (4.2) EC3-1-2 [9].

$$\varepsilon = 0.85\sqrt{235/f_y}$$

2.16

2.8 Design procedure according to Simões da Silva L, Marques L and Rebelo C [10]

Table 2-1 Proposed verification procedure for web-tapered I-section beams according to [10]

Lateral-torsional buckling	
$\alpha_{ult,k}(x_c^I)$	$M_{y,Rk}(x_{c,M}^I)/M_{y,Ed}(x_{c,M}^I)$ – the minimum along the beam, e.g. 10 sections
α_{cr}	Numerically e.g. or by expressions for M_{cr} from literature, see Section 5.2.4. The multiplier α_{cr} shall afterwards be obtained with respect to the applied load.
$\overline{\lambda_{LT}}(x_c^I)$	$\sqrt{\alpha_{ult,k}(x_c^I)/\alpha_{cr}}$
$x_{c,lim}^{II}$	See Table 3
φ_{LT}	For ψ: $\quad A\cdot\psi^2 + B\cdot\psi + C \quad \geq 1$ For UDL: $\quad -0.0025a_\gamma^2 + 0.015a_\gamma + 1.05$ See Table 4 for A,B,C and a_γ
α_{LT}	Hot-rolled: $\quad 0.16\sqrt{\dfrac{W_{y,el}(x_{c,\lim}^{II})}{W_{z,el}(x_{c,\lim}^{II})}} \leq 0.49$ Welded: $\quad 0.21\sqrt{\dfrac{W_{y,el}(x_{c,\lim}^{II})}{W_{z,el}(x_{c,\lim}^{II})}} \leq 0.64$
η_{LT}	$\alpha_{LT}\times\left(\overline{\lambda}_z(x_{c,\lim}^{II})-0.2\right)$ If welded, $\eta_{LT}\leq\sqrt{\dfrac{W_{y,el}(x_{c,\lim}^{II})}{W_{z,el}(x_{c,\lim}^{II})}}\left(0.12\psi^2-0.23\psi+0.35\right)$
$\overline{\lambda}_z(x_{c,lim}^{II})$	$\sqrt{N_{Rk}(x_{c,\lim}^{II})/N_{cr,z,h\min}}$
ϕ_{LT}	$0.5\times\left(1+\varphi\times\eta\times\dfrac{\overline{\lambda}^2{}_{LT}(x_c^I)}{\overline{\lambda}^2{}_z(x_{c,\lim}^{II})}+\varphi\times\overline{\lambda}^2{}_{LT}(x_c^I)\right)$
$\chi_{LT}x_c^I)$	$\varphi\left/\phi+\sqrt{\phi^2-\varphi\times\overline{\lambda}^2{}_{LT}(x_c^I)}\right. \leq 1$
Verification	$\chi_{LT}(x_c^I)\times\alpha_{ult,k}(x_c^I)\geq 1$

Table 2-2 Calculation of $X_{c.lim.M}{}^{II}/L$ for lateral-torsional buckling of tapered I-beams according to [10]

For ψ	$(0.75 - 0.18\psi - 0.07\psi^2) + (0.025\psi^2 - 0.006\psi - 0.06)(\gamma_h - 1) \geq 0$
	If $\psi < 0$ and $\|\psi\|\gamma_w \geq 1 + 1.214(\gamma_h - 1)$, $x_{c,lim}^{II}/L = 0.12 - 0.03(\gamma_h - 1)$
For UDL	$0.5 + 0.0035(\gamma_h - 1)^2 - 0.03(\gamma_h - 1)^2 \leq 0.5$

Table 4: Calculation of φ for lateral-torsional buckling of tapered I-beams

	$\psi < -\psi_{lim}$	$-\psi_{lim} \leq \psi \leq \psi_{lim}$	$\psi > \psi_{lim}$
a_γ	$-0.0005 \cdot (\gamma_w - 1)^4 + 0.009 \cdot (\gamma_w - 1)^3 - 0.077 \cdot (\gamma_w - 1)^2 + 0.78 \cdot (\gamma_w - 1)$		
ψ_{lim}	$1 + 120 \cdot a_\gamma + 600 \cdot a_\gamma^2 - 210 \cdot a_\gamma^3 / 1 + 123 \cdot a_\gamma + 1140 \cdot a_\gamma^2 + 330 \cdot a_\gamma^3$		
φ_{LT}			
A	$-0.0665 \cdot a_\gamma^6 + 0.718 \cdot a_\gamma^5 - 2.973 \cdot a_\gamma^4$ $+5.36 \cdot a_\gamma^3 - 2.9 \cdot a_\gamma^2 - 2.1 \cdot a_\gamma - 1.09$	$\frac{-11.37 + 12090 \cdot a_\gamma - 8050 \cdot a_\gamma^2 + 1400 \cdot a_\gamma^3}{1 - 1058 \cdot a_\gamma + 705 \cdot a_\gamma^2 - 120 \cdot a_\gamma^3} + 11.22$	$0.008 \cdot a_\gamma^2 - 0.08 \cdot a_\gamma - 0.157$
B	$-0.1244 \cdot a_\gamma^6 + 1.3185 \cdot a_\gamma^5 - 5.287 \cdot a_\gamma^4$ $+9.27 \cdot a_\gamma^3 - 5.24 \cdot a_\gamma^2 - 2.18 \cdot a_\gamma - 2$	$+0.02 \cdot a_\gamma^6 - 0.133 \cdot a_\gamma^5 + 0.425 \cdot a_\gamma^4$ $-0.932 \cdot a_\gamma^3 + 1.05 \cdot a_\gamma^2 - 0.5 \cdot a_\gamma - 0.1$	$-0.033 \cdot a_\gamma^3 + 0.04 \cdot a_\gamma^2$ $+0.48 \cdot a_\gamma + 0.37$
C	$-0.0579 \cdot a_\gamma^6 + 0.6003 \cdot a_\gamma^5 - 2.314 \cdot a_\gamma^4$ $+3.911 \cdot a_\gamma^3 - 2.355 \cdot a_\gamma^2 + 0.02 \cdot a_\gamma + 0.3$	$0.02 \cdot a_\gamma^2 - 0.14 \cdot a_\gamma + 1.25$	$0.032 \cdot a_\gamma^3 - 0.092 \cdot a_\gamma^2$ $+0.06 \cdot a_\gamma + 0.8$

Apart from this procedure, in case of beam-column members, it is possible to verify the web-tapered member using interaction formulae given in EC3-1-1 but using some adaptation (explained in [7]).

$$\frac{N_{Ed}}{\chi_y N_{Rk}/\gamma_{M1}} + k_{yy} \frac{M_{y,Ed}}{\chi_{LT} M_{y,Rk}/\gamma_{M1}} \leq 1.0$$

$$\frac{N_{Ed}}{\chi_z N_{Rk}/\gamma_{M1}} + k_{zy} \frac{M_{y,Ed}}{\chi_{LT} M_{y,Rk}/\gamma_{M1}} \leq 1.0$$

2.17

Here, cross section properties to be considered are due to the first order failure location of the axial force acting alone $(x_{c,N}^I)$ for the utilization term regarding axial force; and the first order failure location of the bending moment acting alone $(x_{c,M}^I)$ for the utilization term regarding the bending moment.

As for the interaction factors (k_{yy}, k_{zy}) the equivalent uniform moment factors $C_{m,y}$ and $C_{m,LT}$, Table B.3 of EC3-1-1 should be adopted provided that the diagram to be considered is the <u>bending moment first order utilization diagram</u> instead of the bending moment diagram itself, see Table 2-4.

Table 2-3 Adaptation of the equivalent uniform moment factor Cm for prismatic members [10]
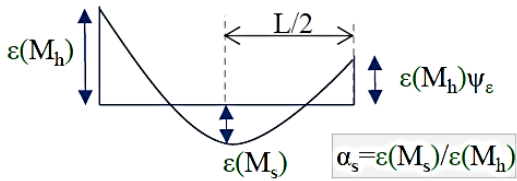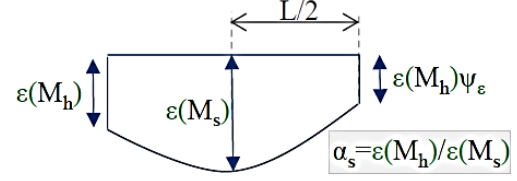
Moment **utilization** diagram	Range		C_{my} and C_{mLT}
$\alpha_s = \varepsilon(M_s)/\varepsilon(M_h)$	$0 \leq \alpha_s \leq 1$	$-1 \leq \psi_\varepsilon \leq 1$	$0.2 + 0.8\,\alpha_s \geq 0.4$
	$-1 \leq \alpha_s < 0$	$0 \leq \psi_\varepsilon \leq 1$	$0.1 - 0.8\,\alpha_s \geq 0.4$
		$-1 \leq \psi_\varepsilon < 0$	$0.1(1-\psi_\varepsilon) - 0.8\,\alpha_s \geq 0.4$
$\alpha_s = \varepsilon(M_h)/\varepsilon(M_s)$	$0 \leq \alpha_s \leq 1$	$-1 \leq \psi_\varepsilon \leq 1$	$0.95 + 0.05\,\alpha_h$
	$-1 \leq \alpha_s < 0$	$0 \leq \psi_\varepsilon \leq 1$	$0.95 + 0.05\,\alpha_h$
		$-1 \leq \psi_\varepsilon < 0$	$0.95 + 0.05\,\alpha_h(1+2\,\psi_\varepsilon)$

Table 2-4 Possible interaction factors for web-tapered beam-columns according to Method 2 [10]

k_{yy}	$C_{my} \times \left(1 + \underbrace{\left(\overline{\lambda}_y(x^{II}_{c,N}) - 0.2 \right)}_{\leq 0.8 \geq 0} \dfrac{N_{Ed}(x^{I}_{c,N})}{\chi_y(x^{I}_{c,N}) N_{Rk}(x^{I}_{c,N})/\gamma_{M1}} \right)$
k_{zy}	$1 - \dfrac{\overbrace{0.1\overline{\lambda}_z(x^{II}_{c,N})}^{\leq 0.1}}{C_{m,LT} - 0.25} \dfrac{N_{Ed}(x^{1}_{c,N})}{\chi_z(x^{1}_{c,N}) N_{Rk}(x^{1}_{c,N})/\gamma_{M1}}$
	$for \; \overline{\lambda}_z(x^{II}_{c,N}) < 0.4$:
	$0.6 + \overline{\lambda}_z(x^{II}_{c,N}) \leq 1 - \dfrac{0.1\overline{\lambda}_z(x^{II}_{c,N})}{C_{m,LT} - 0.25} \dfrac{N_{Ed}(x^{1}_{c,N})}{\chi_z(x^{1}_{c,N}) N_{Rk}(x^{1}_{c,N})/\gamma_{M1}}$

It is suggested to use the interpolation between the reduction factors for flexural and lateral-torsional buckling, respectively χ_z and χ_{LT} to obtain final χ_{op}.

Therefore, for out-of-plane stability verification should be satisfied:

$$\chi_{op} \cdot \alpha_{ult,k} / \gamma_{M1} \geq 1.0 \qquad\qquad 2.18$$

2.9 Class 4 sections

When designing plated structures the effects of shear lag, plate buckling and interaction of the both effects should be taken into account in the global design (EN 1993-1-5).

Therefore, the resistances of the cross sections in this work are determined with their effective sectional properties (if relevant) for both cross section verification and member verification. The effects of shear lag of flanges is taken into account by the use of an effective width and is assumed to be uniform over the length of the beams. The effects of plate buckling are taken into account by effective cross sectional areas of the elements in compression. For the compressed flanges, the combined effect of shear lag and plate buckling are considered.

Eurocode limits the application of the effective width models to members which panels are rectangular and the flanges are parallel, or to non-rectangular members provided that the angel of taper is not greater than 10 degrees. In case this is not fulfilled, the reduction factor should be obtained assuming that the member is of uniform height based on the largest section.

Since the results that were obtained for the members of the short lengths were too conservative even with using the reduction factor based on the critical cross section (which is always smaller than the highest one) this effect is not taken into account.

2.10 Beams at elevated temperature

2.10.1 Resistance of the members

The design moment resistance $M_{fi,\theta,Rd}$ with a uniform temperature θ_a should be determined according to (4.8) in EC3-1-2, which is defined as:

$$M_{fi,\theta,Rd} = k_{y,\theta}[\gamma_{M,0}/\gamma_{M,fi}]M_{Rd} \qquad 2.19$$

where

> M_{Rd} is the plastic moment resistance of the gross cross-section $M_{pl,Rd}$ for normal temperature design, according to EN 1993-1-1 or the reduced moment resistance for normal temperature design, allowing for the effects of shear if necessary, according to EN 1993-1-1;

> $k_{y,\theta}$ is the reduction factor for the yield strength of steel at temperature θ_a

$$M_{b,fi,\theta,Rd} = \chi_{LT,fi} W_y k_{y,\theta,com} f_y / \gamma_{M,fi} \qquad 2.20$$

where

> W_y should be taken as $W_{pl,y}$ in case of cross sections class 1 or 2, while for the classes 3 or 4 it should be taken as $W_{el,y}$;

> $\chi_{LT,fi}$ is the reduction factor for lateral-torsional buckling in the fire design situation;

$k_{y,\theta,com}$ is the reduction factor from section 3 of EC3-1-2 for the yield strength of steel at the maximum temperature in the compression flange $\theta_{a,com}$ reached at time t .

$$\chi_{LT,fi} = \frac{1}{\phi_{LT,\theta,com} + \sqrt{[\phi_{LT,\theta,com}]^2 - [\overline{\lambda}_{LT,\theta,com}]^2}} \qquad 2.21$$

$$\phi_{LT,\theta,com} = \frac{1}{2}[1 + \alpha\overline{\lambda}_{LT,\theta,com} + (\overline{\lambda}_{LT,\theta,com})^2] \qquad 2.22$$

$$\alpha = 0.65\sqrt{235/f_y} \qquad 2.23$$

$$\overline{\lambda}_{LT,\theta,com} = \overline{\lambda}_{LT}[k_{y,\theta,com}/k_{E,\theta,com}]^{0.5} \qquad 2.24$$

where

$k_{E,\theta,com}$ is the reduction factor from section 3 of EC3-1-2 for the slope of the linear elastic range at the maximum steel temperature in the compression flange $\theta_{a,com}$ reached at time t .

2.10.2 Material properties of carbon steel at elevated temperatures

Design values of mechanical (strength and deformation) material properties $X_{d,fi}$ are defined as follows:

$$X_{d,fi} = k_\theta X_k / \gamma_{M,fi} \qquad 2.25$$

where

X_k is the characteristic value of a strength or deformation property (generally f_y or E_k) for normal temperature design to EN 1993-1-1;

k_θ is the reduction factor for a strength or deformation property ($X_{k,\theta}/X_k$), dependent on the material temperature, see section 3 EC3-1-2;

$\gamma_{M,fi}$ is the partial factor for the relevant material property, for the fire situation. This factor for the fire situation is given in the national annex. The use of $\gamma_{M,fi} = 1.0$ is recommended.
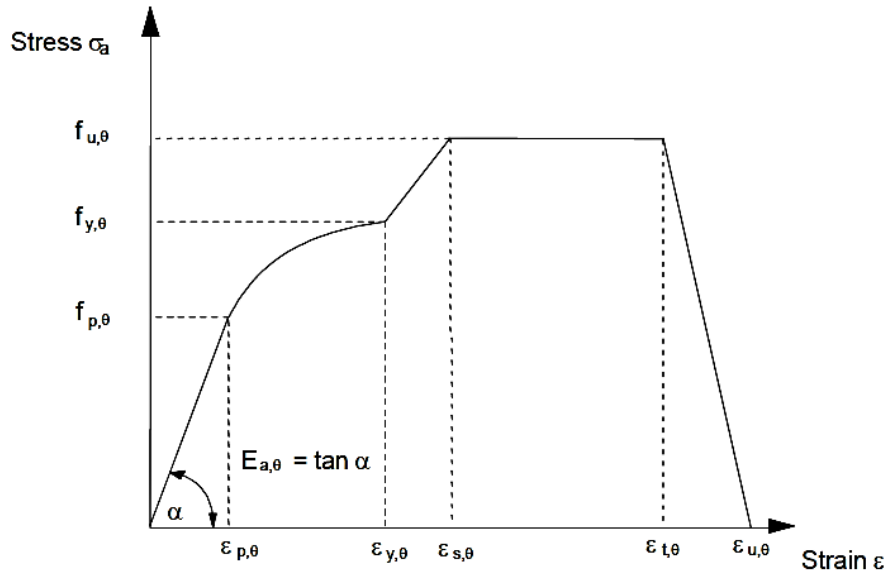
Figure 2-5 Alternative stress-strain relationship for steel allowing for strain-hardening

The detailed explanation on this diagram can be found in Annex A1 of EC3-1-2 [9].

Table 3.1 in EC3-1-2 [9] gives the reduction factors for the stress-strain relationship for steel at elevated temperatures given in *Figure 2-5*. These reduction factors are defined as follows:

- effective yield strength, relative to yield strength at $20°C$: $k_{y,\theta} = f_{y,\theta} / f_y$

- proportional limit, relative to yield strength at $20°C$: $k_{p,\theta} = f_{p,\theta} / f_y$

- slope of linear elastic range, relative to slope at $20°C$: $k_{E,\theta} = E_{a,\theta} / E_a$.

Table 2-5 Reduction factors for stress-strain relationship of carbon steel at elevated temperatures, EC3, Part 1-2: General rules -Structural fire design

Steel Temperature θ_a	Reduction factors at temperature θ_a relative to the value of f_y or E_a at 20°C		
	Reduction factor (relative to f_y) for effective yield strength $k_{y,\theta} = f_{y,\theta}/f_y$	Reduction factor (relative to f_y) for proportional limit $k_{p,\theta} = f_{p,\theta}/f_y$	Reduction factor (relative to E_a) for the slope of the linear elastic range $k_{E,\theta} = E_{a,\theta}/E_a$
20°C	1,000	1,000	1,000
100°C	1,000	1,000	1,000
200°C	1,000	0,807	0,900
300°C	1,000	0,613	0,800
400°C	1,000	0,420	0,700
500°C	0,780	0,360	0,600
600°C	0,470	0,180	0,310
700°C	0,230	0,075	0,130
800°C	0,110	0,050	0,090
900°C	0,060	0,0375	0,0675
1000°C	0,040	0,0250	0,0450
1100°C	0,020	0,0125	0,0225
1200°C	0,000	0,0000	0,0000

3 Evaluation of the numerical model

In order to perform numerical analysis, a finite element model was implemented using the commercial finite element package Abaqus (version 6.11).

3.1 Structural elements

Since the stresses in the thickness direction are negligible, the beams are modelled with linear 4 node shell elements S4. Three-dimensional shell elements have six degrees of freedom at each node (three translations and three rotations).The stresses and strains are calculated via numerical integration independently at each section point (integration point) through the thickness of the shell, thus allowing nonlinear material behaviour. Abaqus shell elements assume that plane sections perpendicular to the plane of the shell remain plane. This means that an elastic-plastic shell may yield at the outer section points while remaining elastic at the inner section points. Effects of transverse shear deformation are taken into account by defining shell elements as thick. Hence, material lines that are initially normal to the shell surface do not necessarily remain normal to the surface throughout the deformation, thus adding transverse shear flexibility.
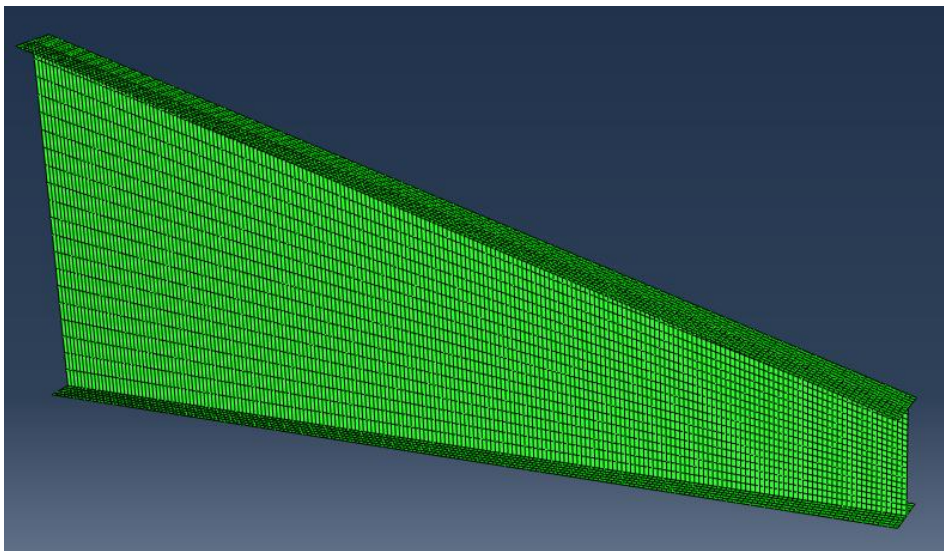
Figure 3-1 Numerical model

3.3 Analysis types

Both Linear Eigenvalue Analysis and Geometrical and Material Non-linear Analysis are carried out. Typical buckling shape of a beam is presented in the picture below.
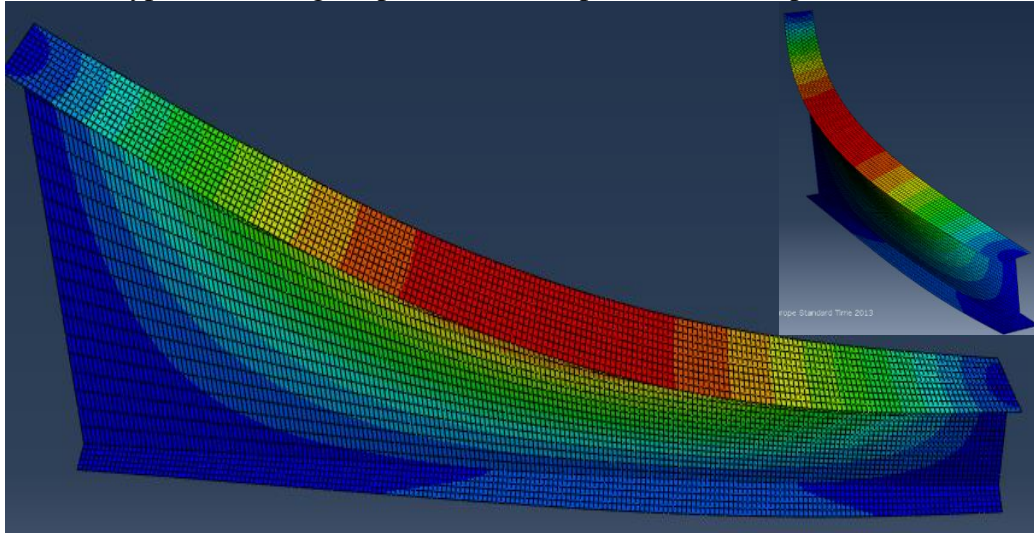

Figure 3-2 Buckling shape

3.4 Material properties

Steel grade S355 was used in reference examples, with a yield stress $f_y = 355 MPa$. Material is set to be elastic-perfectly plastic with the modulus of elasticity $E = 210 GPa$, and a Poison's ration of $\nu = 0.3$.

In the finite element model, the elastic-plastic material properties are considered, taking into account the strain hardening. The properties of the steel are redefined according to the temperature level. Here is presented the basic stress-strain diagram for the room temperature.
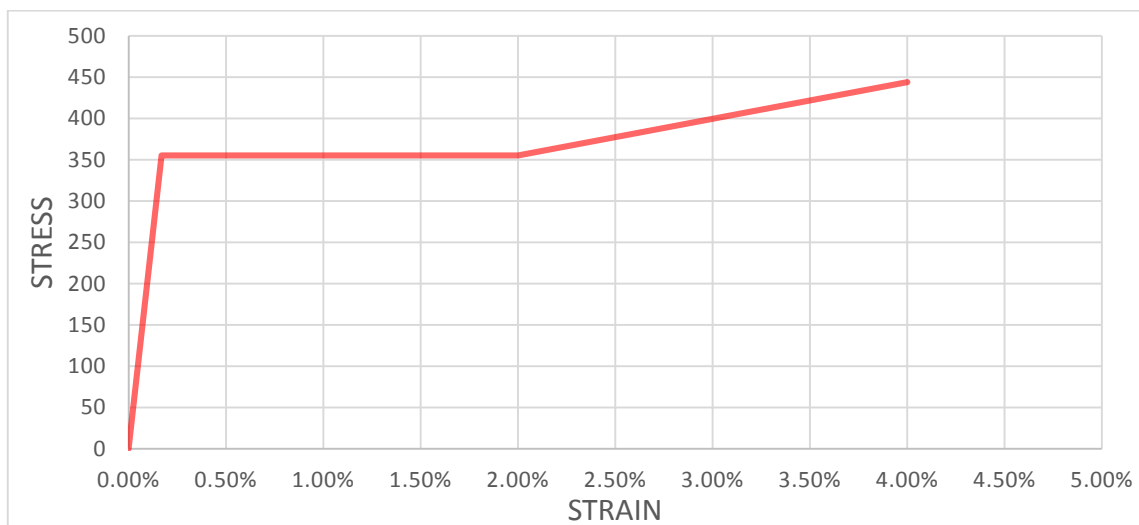
Graph 3-3 Stress-Strain diagramwith linear strain hardening for the room temperature

3.5 Geometrical and material imperfections

Shape and magnitude of imperfections are one of the main difficulties that one encounters when dealing with tapered members.

As for the numerical analysis, geometrical imperfections are defined to be proportional to the eigenmode deflection.

$$\delta_0(x) = \delta_{cr}(x) \cdot \overline{e}_0 \qquad\qquad 3.1$$

EC3-1-5 gives the guidance for the implementation of the imperfections in FE-model (see [11], Annex C.5). Here it says that for the geometric imperfections equivalent geometric imperfections may be used. Equivalent geometric imperfections that take into account the effects of:
- geometrical imperfections of members as governed by geometrical tolerances in product standards or the execution standard;
- structural imperfections due to fabrication and erection;
- residual stresses;
- variation of the yield strength.

Maximal fabrication tolerances are given in the Annex D of EN 1090-2. 80 % of the geometric fabrication tolerances is recommended by EN 1993-1-5.

This would lead to:
- global imperfections

$$\delta_{0,gl}(x) = 80\% [\delta_{cr}(x) \cdot \overline{e}_0] = \delta_{cr}(x) \cdot \frac{0.8L}{750} \qquad\qquad 3.2$$

- local imperfections

$$\delta_{0,gl}(x) = 80\% [\delta_{cr}(x) \cdot \overline{e}_0] = \delta_{cr}(x) \cdot \frac{0.8 \cdot b}{100} \qquad\qquad 3.3$$

Table 3-1 Equivalent geometric imperfections according to EN 1993-1-5

Type of imperfection	Component	Shape	Magnitude
global	member with length ℓ	bow	see EN 1993-1-1, Table 5.1
global	longitudinal stiffener with length a	bow	min ($a/400$, $b/400$)
local	panel or subpanel with short span a or b	buckling shape	min ($a/200$, $b/200$)
local	stiffener or flange subject to twist	bow twist	1 / 50

In combining imperfections a leading imperfection should be chosen and the accompanying imperfections may have their values reduced to 70%.

Since tapered members are usually of class 4 webs, web buckling is allowed.

Also, residual stresses are taken into account when performing numerical analysis. In cases of elevated temperatures, the residual stresses are reduced together with the yield strength of the material accordingly.
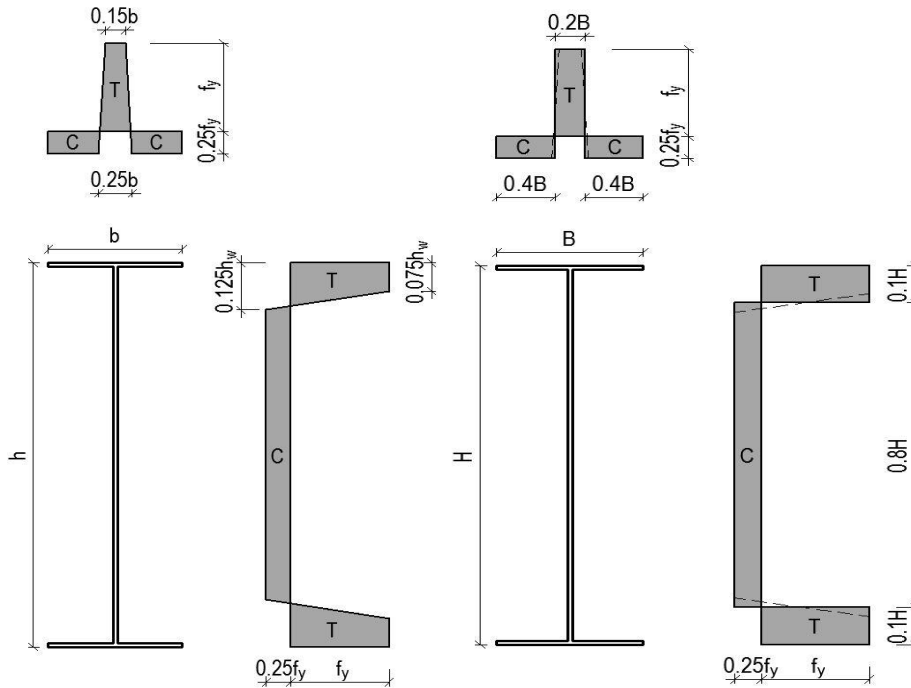
Figure 3-4 Distribution of residual stress in I welded section (C-compression; T – tension)(a), and the actual residual stress stress pattern (simplification for Abaqus) (b)

3.6 Boundary conditions of the model

Modelling of plane sections of solid elements has to be defined so that even after the deformation of the member, the planes remain planar. The relative motion between the nodes on the boundary is required. One of the possible ways to define this type of boundary conditions is either by defining linear constraint equations or by coupling of the restraints.

A linear multi-point constraint requires that a linear combination of nodal variables is equal to zero. Differently saying: $A_1 u_i^P + A_2 u_j^Q + ... + A_N u_k^R = 0$, where u_i^P is a nodal variable at node *P*, degree of freedom *i* and the A_N are coefficients that define the relative motion of the nodes. The first model that was made had the boundary conditions defined in this way, but in the final version of the numerical model the coupling of restraints is chosen since it seemed to be more appropriate even though the obtained results didn't vary much.

Kinematic coupling constraints limit the motion of a group of nodes to the rigid body motion. The surface-based coupling constraint couples the motion of a collection of nodes on a surface to the motion of a reference node. The reference node in this case are set to be the point of the middle of the web's beginning and web's end as well as middle of the flanges' beginnings and ends. This is because the neutral axis of the member is defined to be the middle line of the member. This kinematic coupling constraint does not allow relative motion among the constrained DOFs. For this, all the DOFs are constrained.
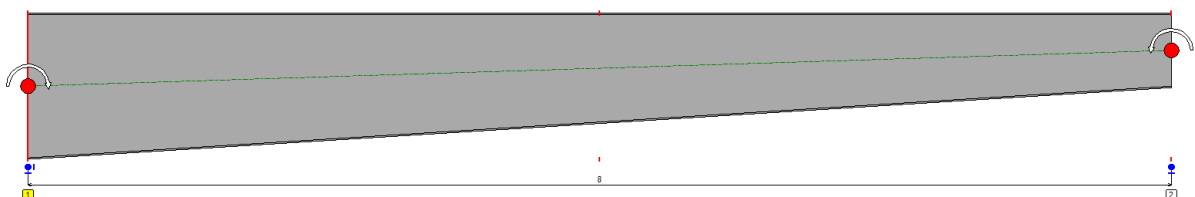
4 Parametric study

Table 4-1 is presenting the characteristics of the cross sections that have been analyzed within this study. As can be seen, two beams have been chosen for computer simulation purposes.

Table 4-1 Definition of the analysed beams type 1(a) and beams type 2 (b)

a)	Left End	Right End
h.w (mm)	1000	500
t.w (mm)	5	5
t.f (mm)	10	10
b.f (mm)	300	300
i0 (mm)	425.53	239.43
Iz (cm4)	4501	4500.5
It (cm4)	23.81	21.73
Iw (cm6)	1.15E+07	2.93E+06
A (mm2)	11000	8500
Av.y (mm2)	6000	6000
Av.z (mm2)	5050	2550
Iy (cm4)	194687	44228
Wel.y (cm3)	3817.4	1701.1
Wel.z (cm3)	300.07	300.03
Wpl.y (cm3)	4280	1842.5
Wpl.z (cm3)	456.25	453.13

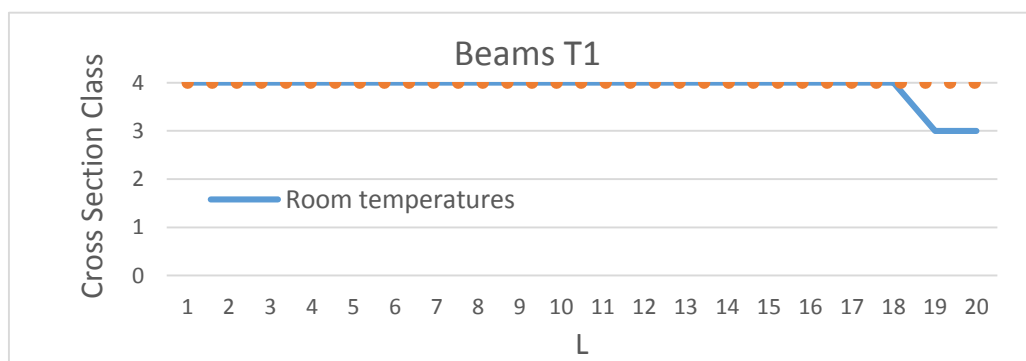| b)	Left End	Right End
h.w (mm)	2000	500
t.w (mm)	10	10
t.f (mm)	20	20
b.f (mm)	300	300
i0 (mm)	770.52	243.24
It (cm4)	9016.7	9004.2
It (cm4)	221.04	171.04
Iw (cm6)	9.20E+07	6.09E+06
A (mm2)	32000	17000
Av.y (mm2)	12000	12000
Av.z (mm2)	20200	5200
Iy (cm4)	1.89E+06	91577
Wel.y (cm3)	18538	3391.7
Wel.z (cm3)	601.11	600.28
Wpl.y (cm3)	22120	3745
Wpl.z (cm3)	950	912.5

Figure 4-1 Cross Section Class along the length of the beams T1 at both room and elevated temperatures
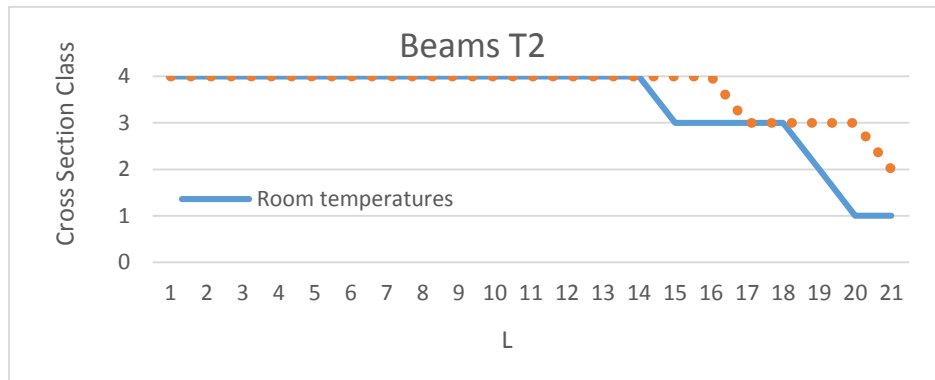
26

Figure 4-2 Cross Section Class along the length of the beams T2 at both room and elevated temperatures

As for the beams of type 1 (further T1), the ratio of the heights is $\gamma_h = 2$ and the ratio of the elastic section modulus at the beginning and the end of the beams is $\gamma_w = 2,211$. Beam of type 2 (further T2) have the ratio of the heights is $\gamma_h = 4$ while the ratio of the elastic section modulus at the beginning and the end of the beams is $\gamma_w = 2,211$.

For the computation of the elastic critical load, Linear Buckling Analysis are performed. Since both of the beams are slender, the global buckling shape of shorter beams is obtained by introducing proportionally thicker web and flanges of the member. In this way any plate buckling and distortions of the section were disregarded.

When defining the cross section class, 10 locations of an element were checked. According to the cross section class, the utilization ration was calculated at each of this location which gave the location of the first order failure (the position of the maximum utilization defines to the first order failure cross section).
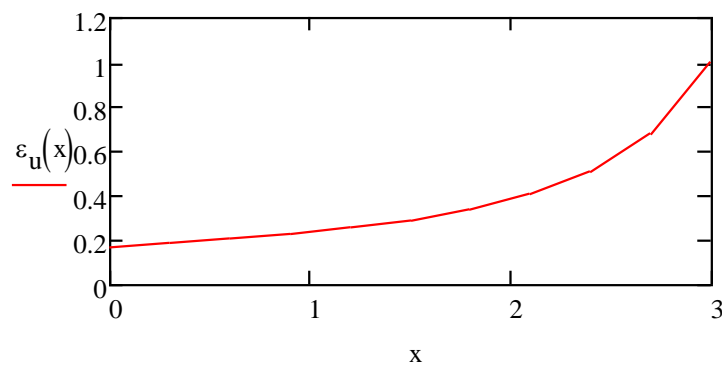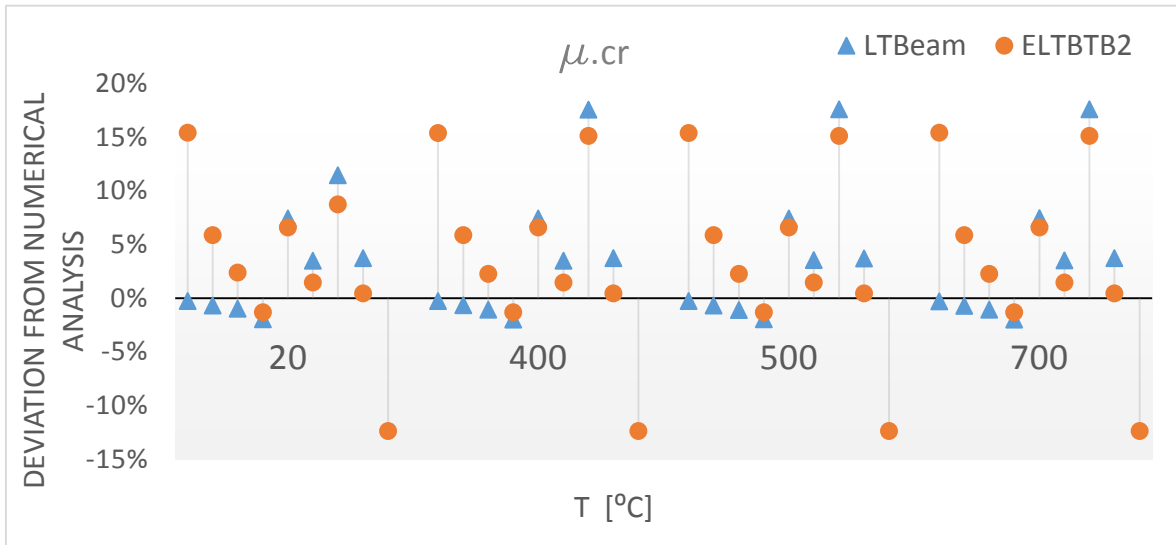

*Figure 4-3 Cross section utilization*

4.1 Elastic critical moment

Here below are presented the results for the elastic critical moment obtained by different software for the observed beams.

In this case the models are run in Abaqus, and the results are compared with the results obtained by LTBeamN as well as ELTBTB2 software.
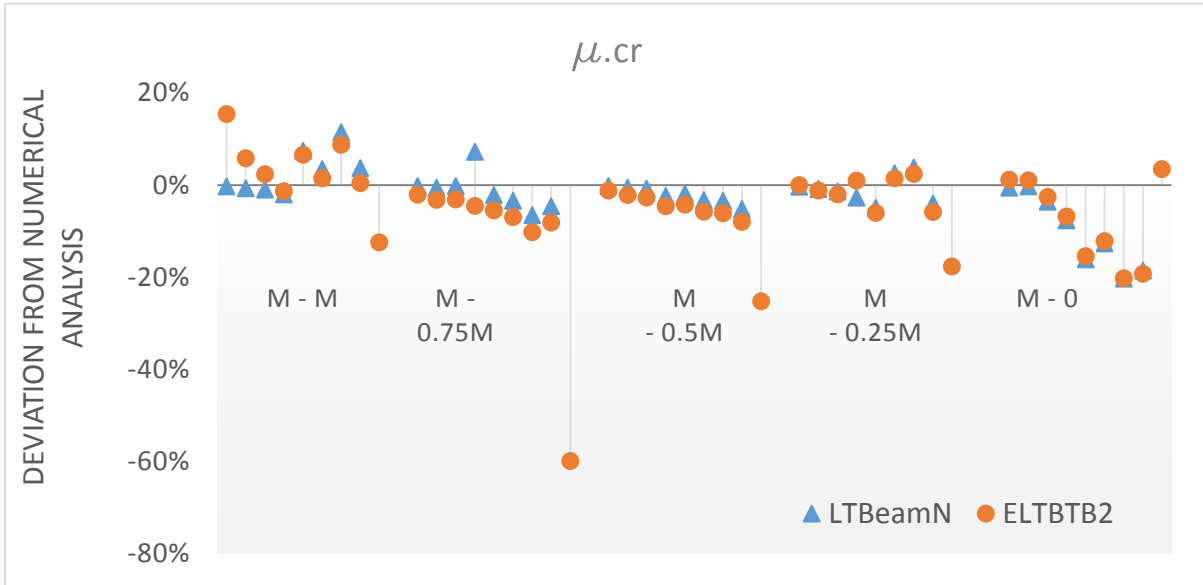
Graph 4-2 Daviation of critical amplifier for diferent temperatures, beams T1, uniform bending moment distribution
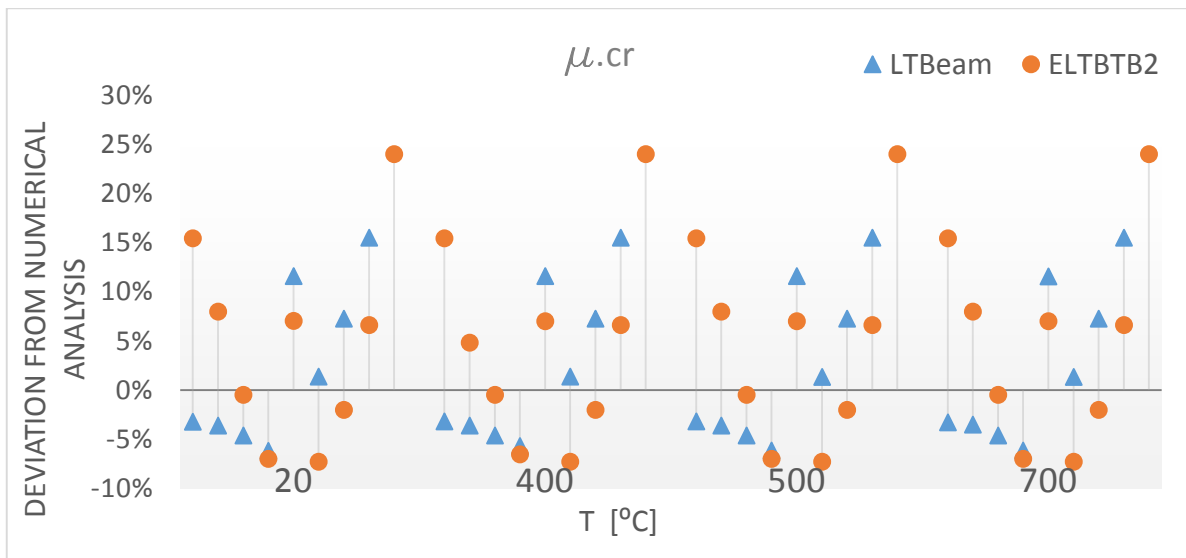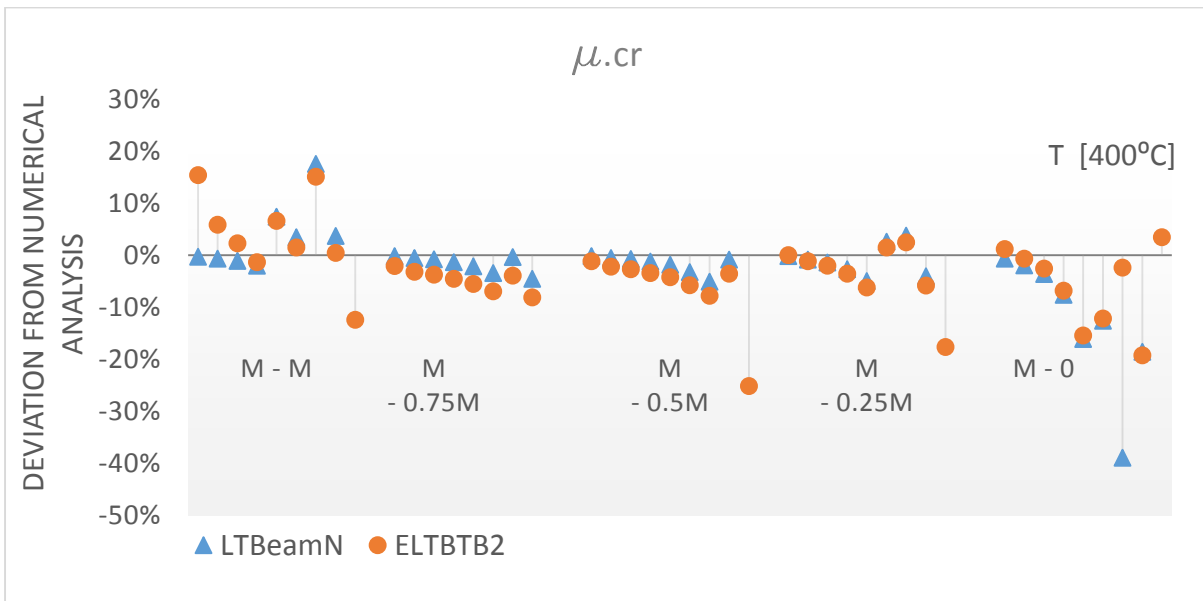

Graph 4-3 Daviation of critical amplifier for diferent temperatures, beams T2, uniform bending moment distribution

It can be seen from the graphs that the results obtained by LTBeamN really well corresponds to the numerical ones. The differences are in the range from -5% to +10%. But in the cases of very slender beams, with the slenderness bigger than 2, the critical moment obtained by LTBeamN is much higher than the real one (difference around 15%). Similar is with the beams with very low slenderness, below 0.3, when the difference is sometimes around 20%.
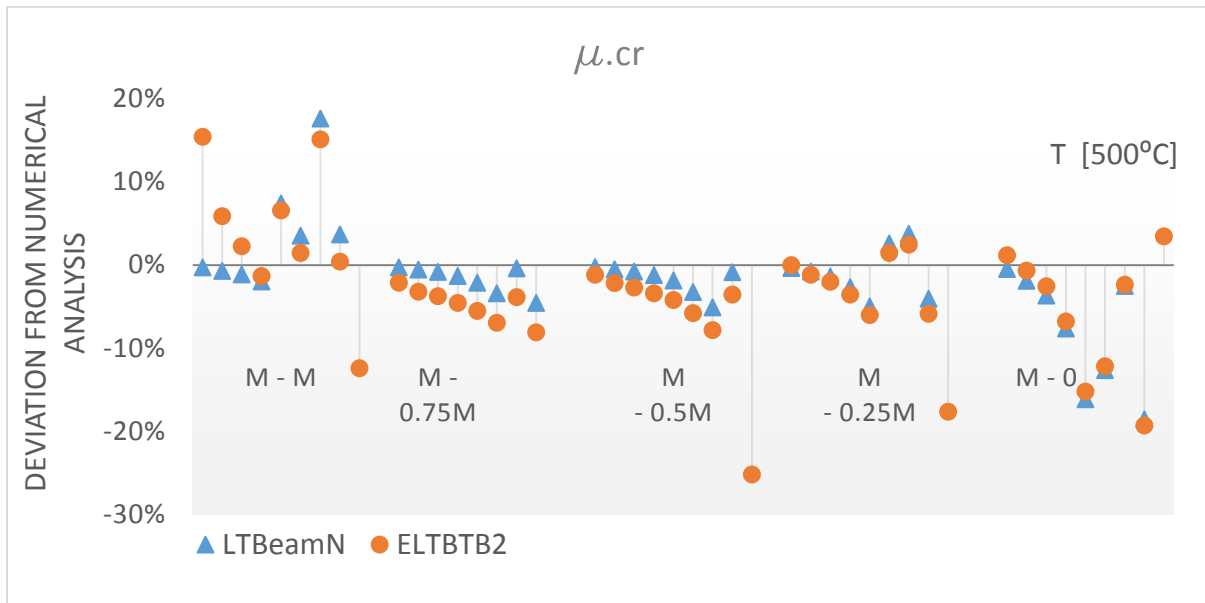
Here below are presented the graphs for deviation of the results in respect to the load distribution.
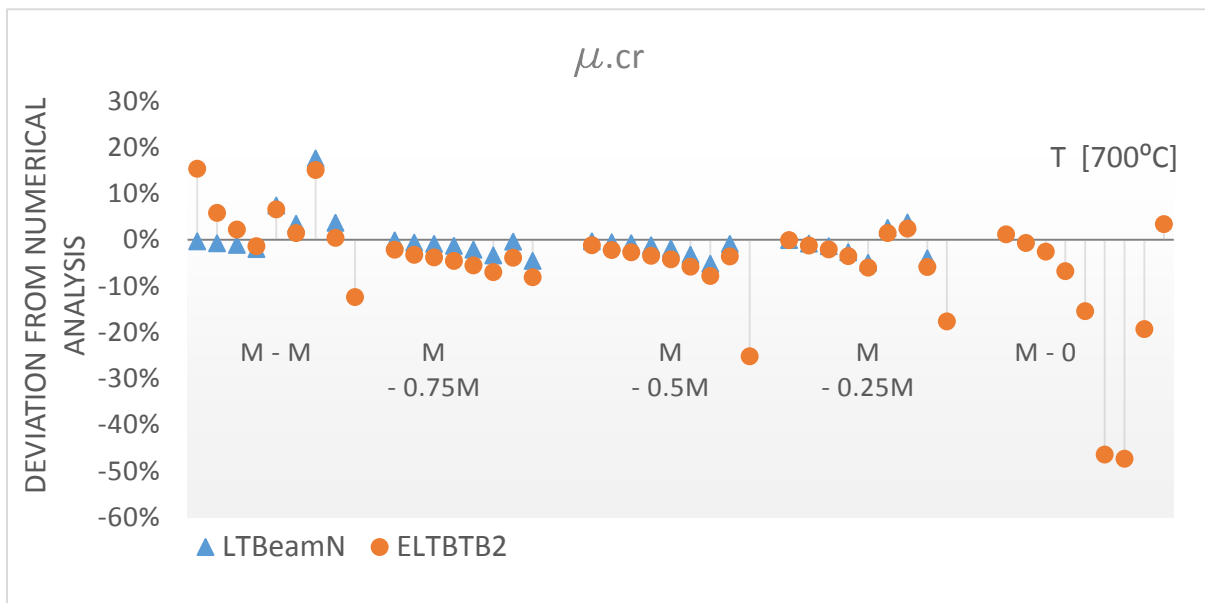

Graph 4-4 Daviation of critical amplifier for load distribution, beams T1, room temperature
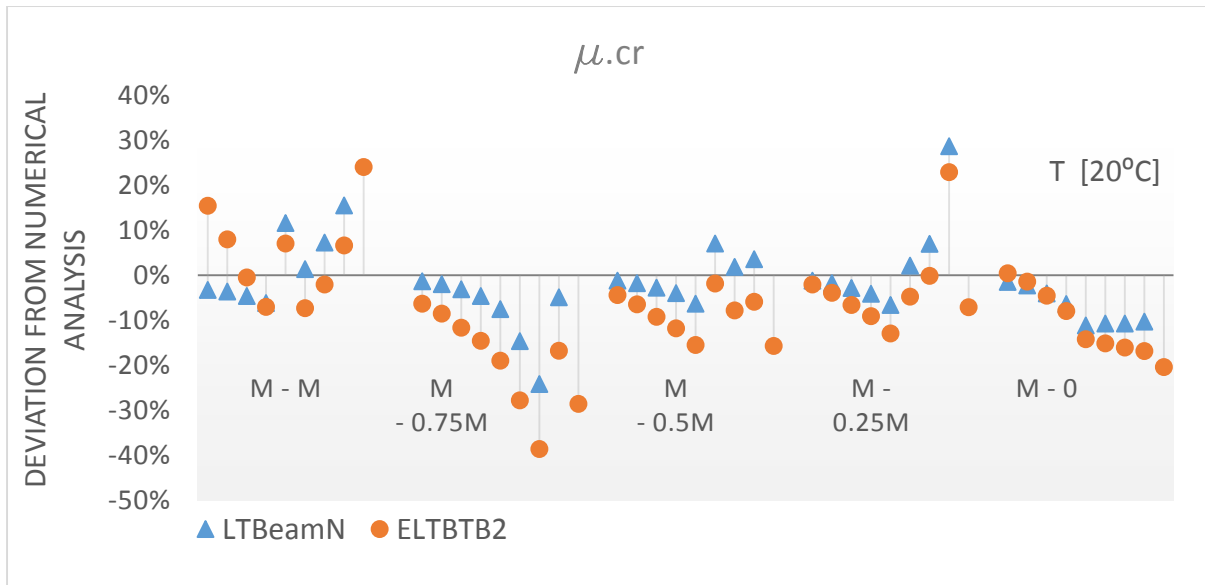

Graph 4-5 Daviation of critical amplifier for load distribution, beams T1, 400 ^0C
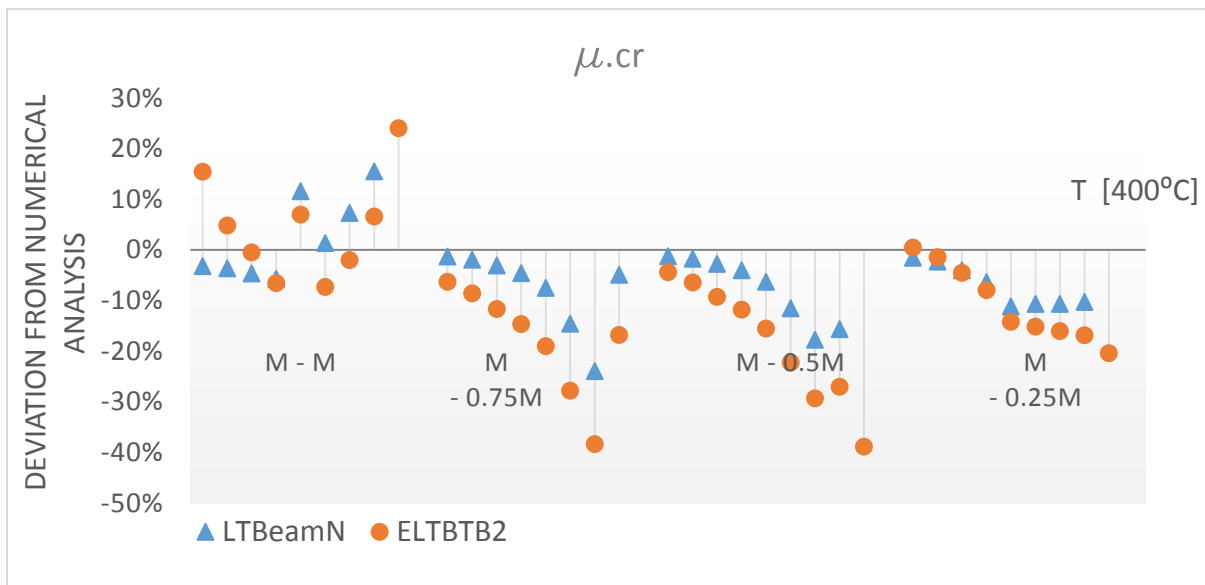
Graph 4-6 Daviation of critical amplifier for load distribution, beams T1, 500 ⁰C

Graph 4-7 Daviation of critical amplifier for load distribution, beams T1, 700 ⁰C

Graph 4-8 Daviation of critical amplifier for diferent load distribution, beams T2, room temperature

Graph 4-9 Daviation of critical amplifier for diferent load distribution, beams T2, 400 ^{0}C
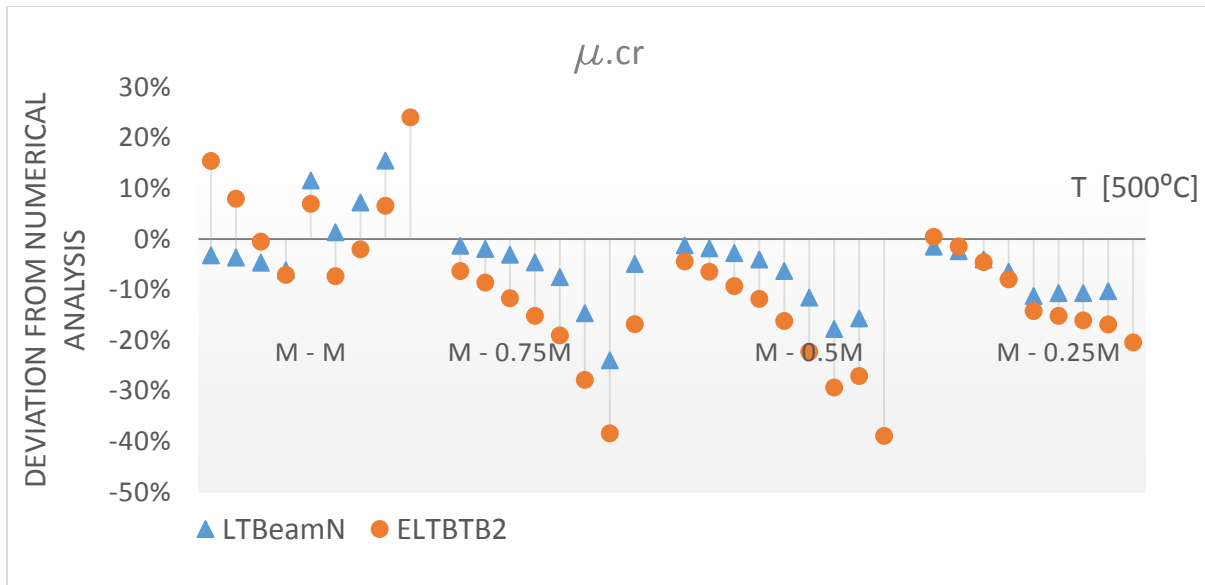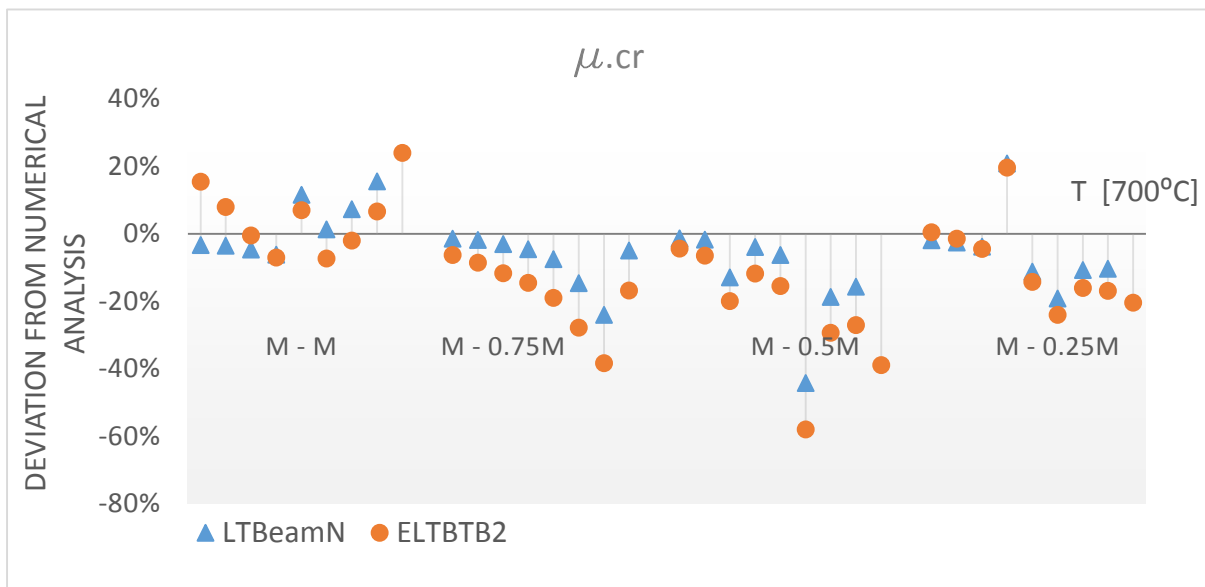
Graph 4-10 Daviation of critical amplifier for diferent load distribution, beams T2, 500 ^0C

Graph 4-11 Daviation of critical amplifier for diferent load distribution, beams T2, 700 ^0C

4.2 Resistance of the cross section

In this study, cross section resistance was evaluated by performing geometrical and material non-linear analysis in Abaqus and the obtained results were compared to the ones obtained by using Marques Liliana's design procedure explained in [3] as well as Merchant-Rankine procedure suggested by Marc Braham and Dominique Hanikenne in [12]. This results were also compared with the ones calculated by using buckling curves given in EN 1993-1-1 for the design of steel structures and EN 1993-1-2 for the fire design.

4.2.1 Merchant-Rankine

Even though the work of Braham and Hanikenne was limited to beams with no plate buckling, no distortion of the cross section and to a linear diagram of bending moment, in this work it has been extended to cross sections of class 4.

Relative slenderness is defined as:

$$\overline{\lambda}_{LT} = \sqrt{\frac{\mu_p}{\mu_{cr}}} \, , \tag{4.1}$$

where μ_p and μ_{cr} are 'multiplicators' of the <u>plastic banding capacity</u> in the <u>weakest section</u> of the beam and attainment of the elastic lateral instability of the beam respectively. Even though this concept of the amplifiers is present even in Eurocode, the reduction of the bending capacity of the beam is defined in a different way:

$$\chi_{LT} = \left(\frac{1}{1 + \overline{\lambda}_{LT}^{2n}}\right)^{1/n} . \tag{4.2}$$

Here factor n depends on the angle of taper and has been shown that the suggestion given in [12] which says that in the case of constant bending moment it can be assumed to be equal to 1.5, gives too conservative results. Therefore, new values for this coefficient have been investigated and the results are presented in the graphs below (starting with the *Graph 4-15*).

Since the beams that were investigated in this research are of class 4, instead of plastic resistance of the section, the elastic ones were used in order to stay consistent with the rules given in Eurocode. As for the critical multiplier, the results obtained by the elastic buckling FEA were used.

The most suitable value for the exponent n is chosen to be the value of γ_w in case of room temperatures while for the elevated temperatures this value should be smaller. For this case, n being equal to 1.5, as it was originally suggested, gave the best results in comparison with the numerical results.

4.2.2 Marques Liliana's approach

Even though this analytical model was calibrated for the beams class 1 and 2, here has been applied on the beams of class 4.

It has been seen that the best results are obtained when the cross section class is defined according to the highest class within the member. This means that even though the class of the smallest section in case of beams T2 is 1 or 2, the elastic effective properties were used.

As for the resistance of the cross section in the case of elevated temperatures, this approach gives mostly unsafe results even without using the over-strength factor. Here, when

defining the slenderness, plastic section properties were used when relevant. In this case the results are closer to the ones obtained numerically, but still unsafe.

4.2.3 Eurocode approach for the access stability of members
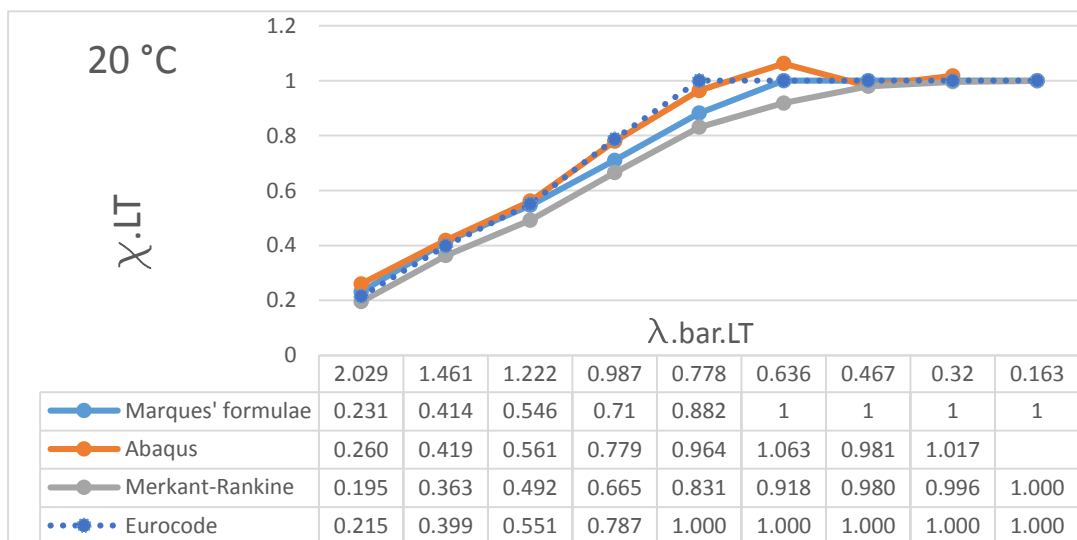
Annex B of EN 1993-1-5 gives rules for defining the reduction factor for the member resistance in case of non-uniform members. Imperfection factor to be used is $\alpha_p = 0.34$ and $\overline{\lambda}_{p0} = 0.8$ (in case of welded profiles) instead of α_{LT} and $\overline{\lambda}_{p0} = 0.2$ as it is according EN 1993-1-1.

Table 4-12 Values for α_p and λ_{p0}, EN 1993-1-5

Product	predominant buckling mode	α_p	$\overline{\lambda}_{p0}$
hot rolled	direct stress for $\psi \geq 0$	0,13	0,70
	direct stress for $\psi < 0$		0,80
	shear		
	transverse stress		
welded or cold formed	direct stress for $\psi \geq 0$	0,34	0,70
	direct stress for $\psi < 0$		0,80
	shear		
	transverse stress		

4.3 Results

↓ Reduction factor

	2.029	1.461	1.222	0.987	0.778	0.636	0.467	0.32	0.163
Marques' formulae	0.231	0.414	0.546	0.71	0.882	1	1	1	1
Abaqus	0.260	0.419	0.561	0.779	0.964	1.063	0.981	1.017	
Merkant-Rankine	0.195	0.363	0.492	0.665	0.831	0.918	0.980	0.996	1.000
Eurocode	0.215	0.399	0.551	0.787	1.000	1.000	1.000	1.000	1.000

Graph 4-13 Reduction factor – slenderness diagram, beams T1, uniform bending moment distribution

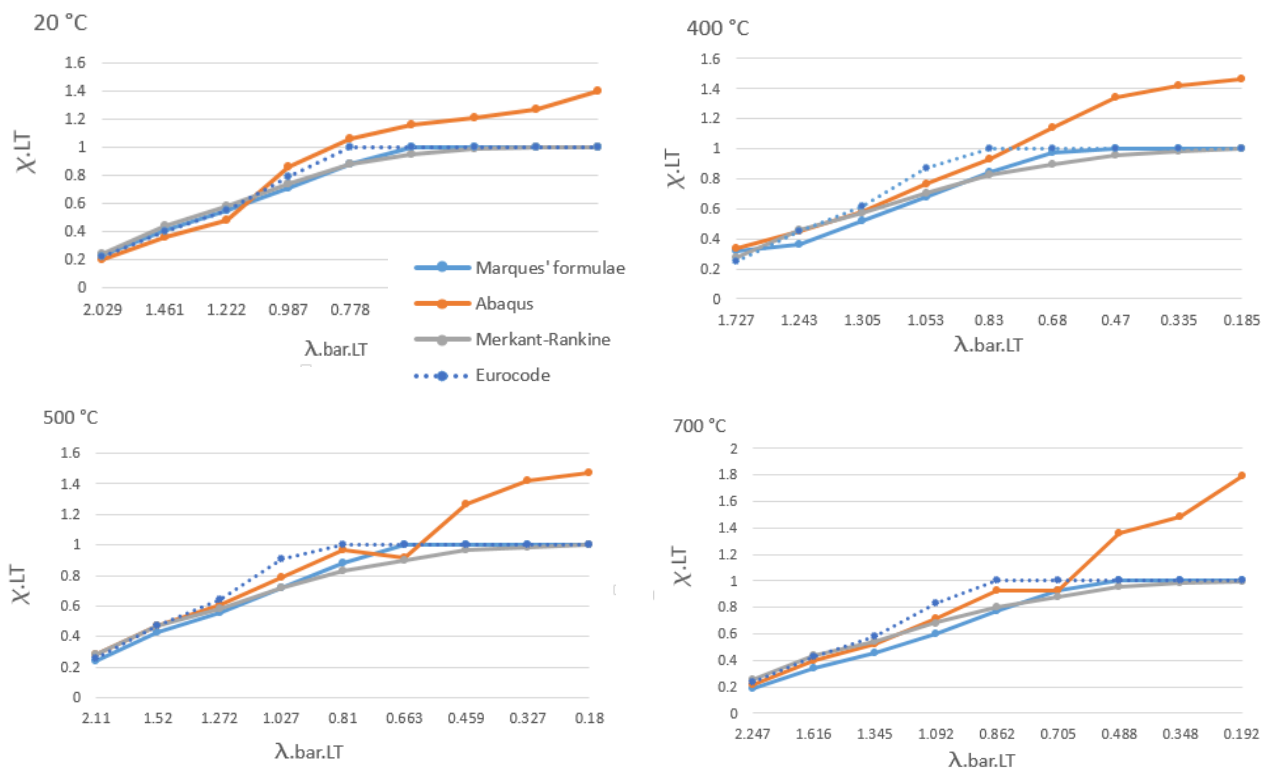| λ.bar.LT	1.594	1.386	1.159	0.996	0.743	0.597	0.484	0.370	0.250
Marques' formulae	0.369	0.471	0.629	0.775	1	1	1	1	1
Abaqus	0.388	0.489	0.665	0.861	1.038	1.022	1.024	1.036	0.967
Merkant-Rankine	0.393	0.518	0.720	0.884	0.993	0.999	1.000	1.000	1.000
Eurocode	0.339	0.439	0.605	0.775	1.000	1.000	1.000	1.000	1.000
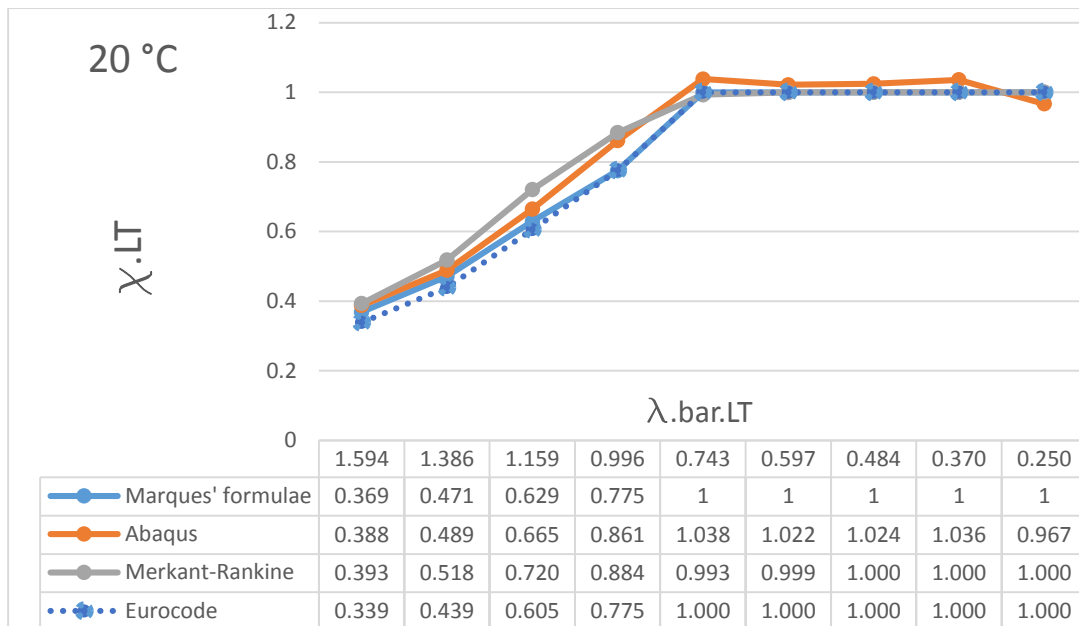
Graph 4-14 Reduction factor – slenderness diagram, beams T2, uniform bending moment distribution

Graph 4-15 Reduction factor due to various approaches for different temperatures, beams T1, uniform bending moment distribution
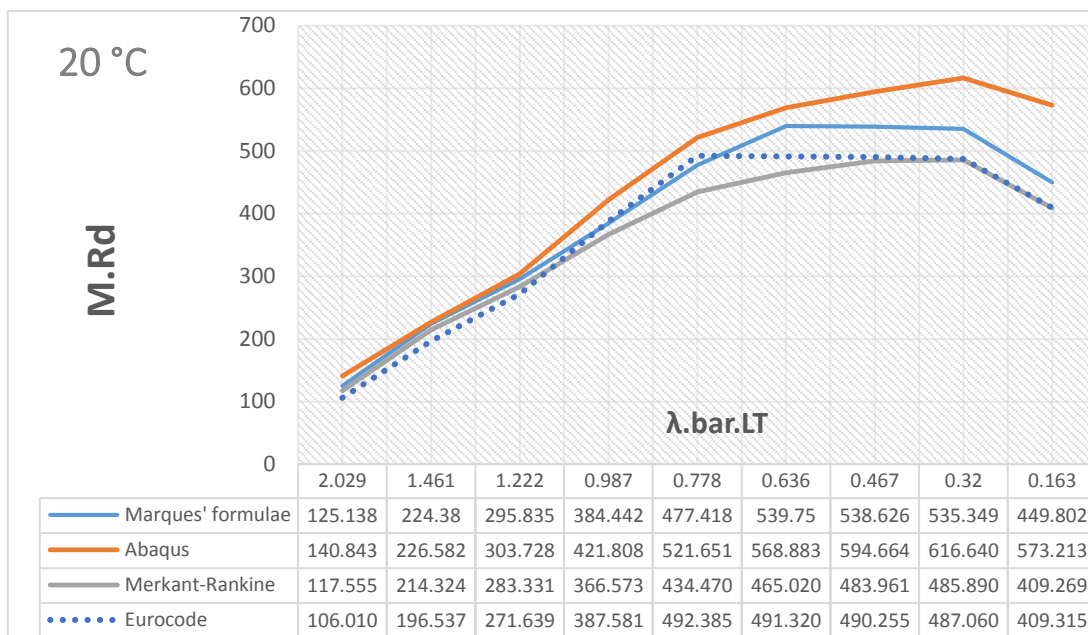
Here it can be seen that both Merkant-Rankine's and Marques' approaches give safe results which very well correspond to the numerical ones. The deviation in the results for the slenderness lower than 0.5 is due to the fact that the resistance of the beam is not achieved by lateral torsional buckling, and this cases (section resistance) are not studied in this research. The two studied approaches at room temperatures give almost the same results. The two curves in the first graph are matching almost completely but still giving slightly unsafe results for the slenderness bigger than 1.0.
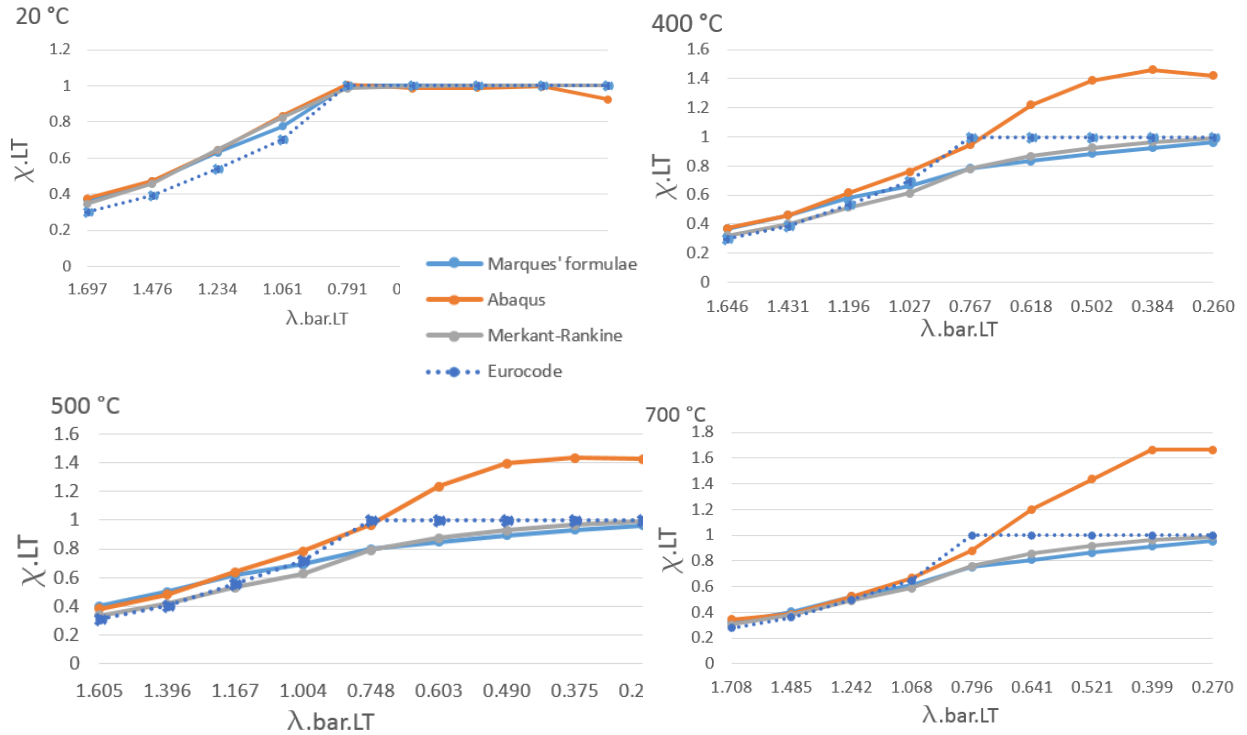
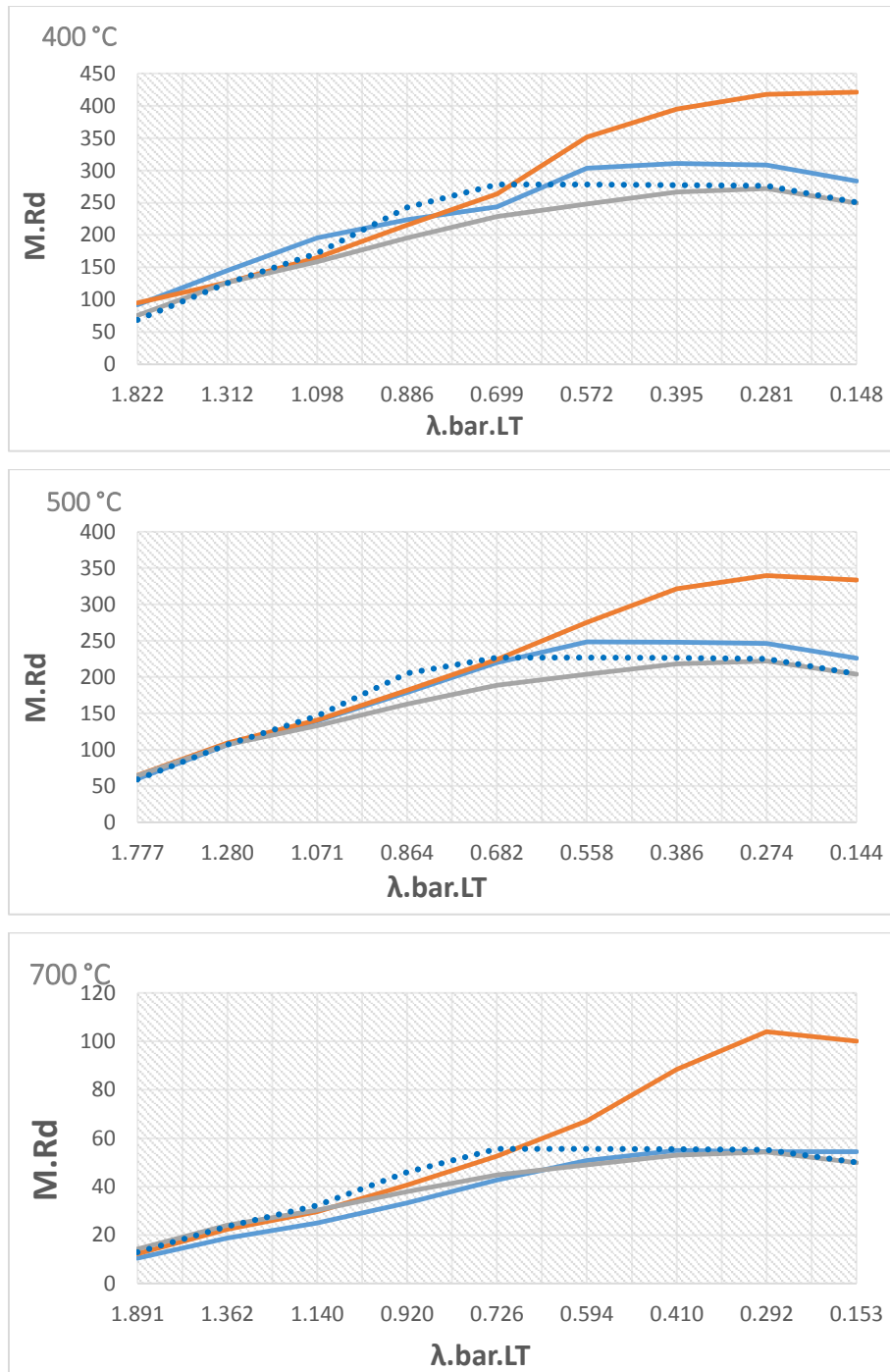*Graph 4-16 Reduction factor due to various approaches for different temperatures, beams T2*

Here in the first graph on the top can be seen that all the results match very well. This is due to the fact that the critical section of the beams is not of class 4. This result actually just verifies the accuracy of the existing procedures. Even the Eurocode procedure is corresponding well to the numerical results.

Cross section resistance

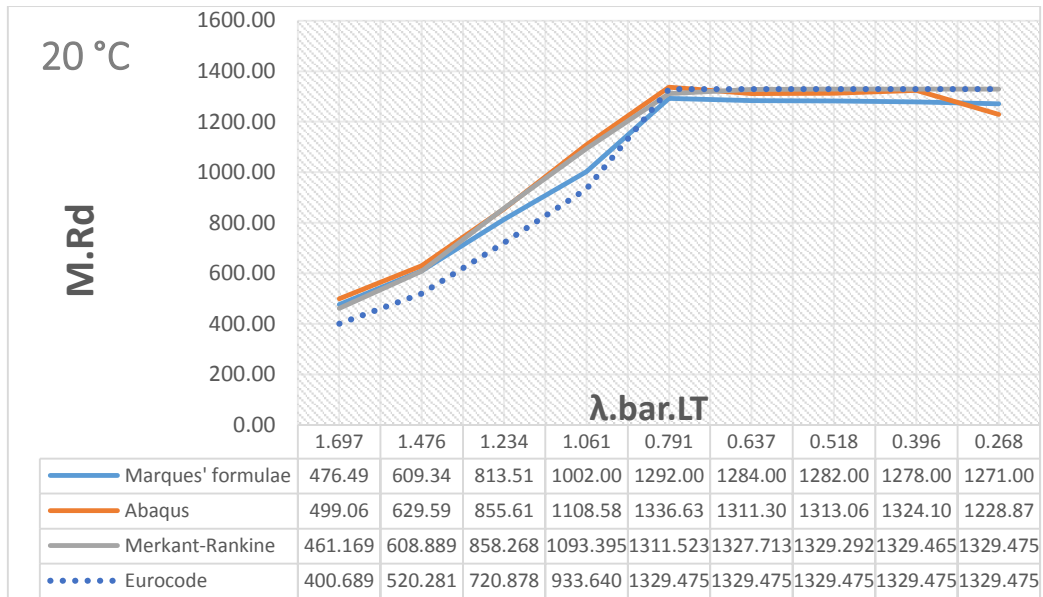|	2.029	1.461	1.222	0.987	0.778	0.636	0.467	0.32	0.163
Marques' formulae	125.138	224.38	295.835	384.442	477.418	539.75	538.626	535.349	449.802
Abaqus	140.843	226.582	303.728	421.808	521.651	568.883	594.664	616.640	573.213
Merkant-Rankine	117.555	214.324	283.331	366.573	434.470	465.020	483.961	485.890	409.269
Eurocode	106.010	196.537	271.639	387.581	492.385	491.320	490.255	487.060	409.315

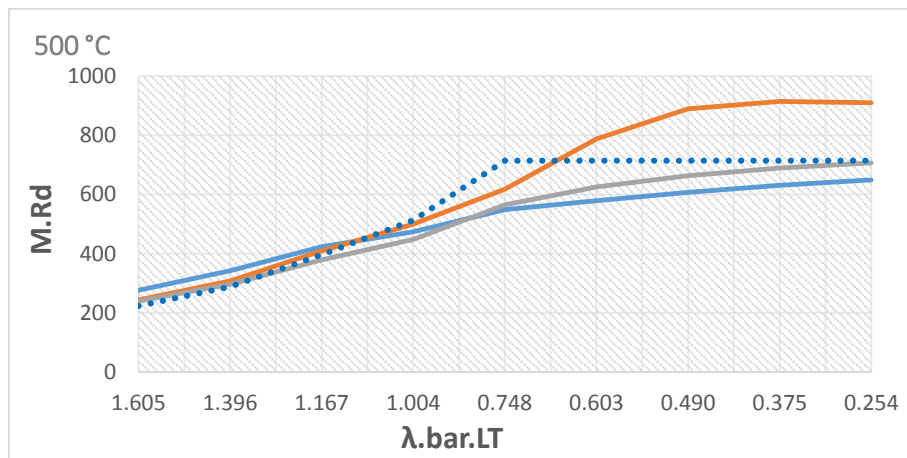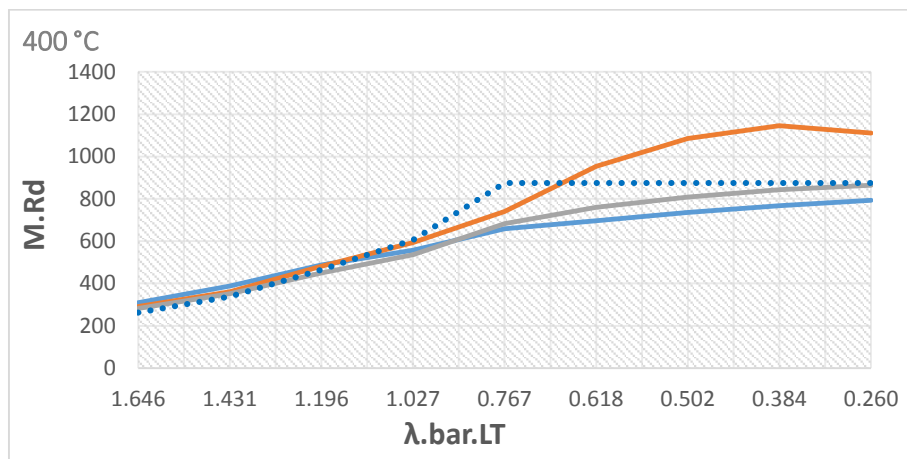*Graph 4-17 Daviation of section resistance of beams T1, room temperature*

In the case of beams type T1, the results obtained by Marques' equations differ from the numerical ones more than in the case of beams type T2. This is because at the position of the critical section in case of beams T2, the cross sections are of class 1 or 2 which are the cases that Marques' approach is calibrated at. Still, in this condition of Class 4, this procedure gives very good results. It should be said that in the graph presented above (*Graph 4-18*) the resistances of beams that have slenderness lower than 0.5 are governed by local buckling of the plates and more importantly also affected by shear forces. This causes the decrease in resistance in the chart for short beams.
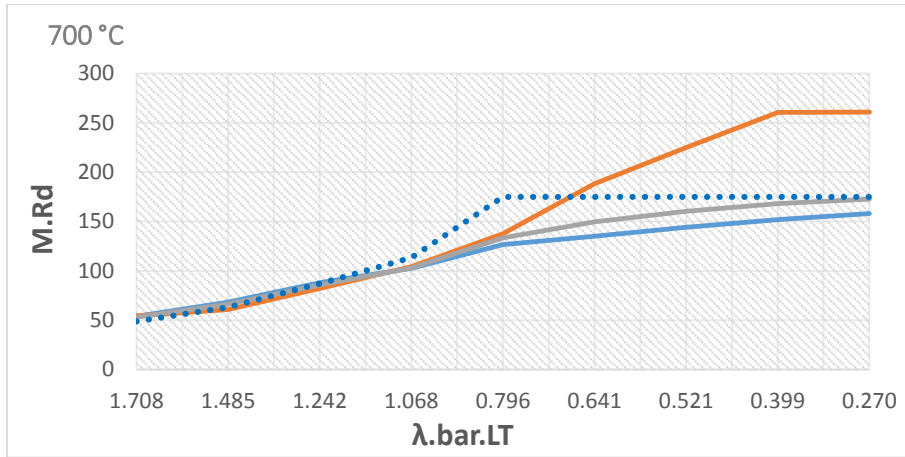
Graphs 4-19 Daviation of section resistance of beams T1, various temperatures
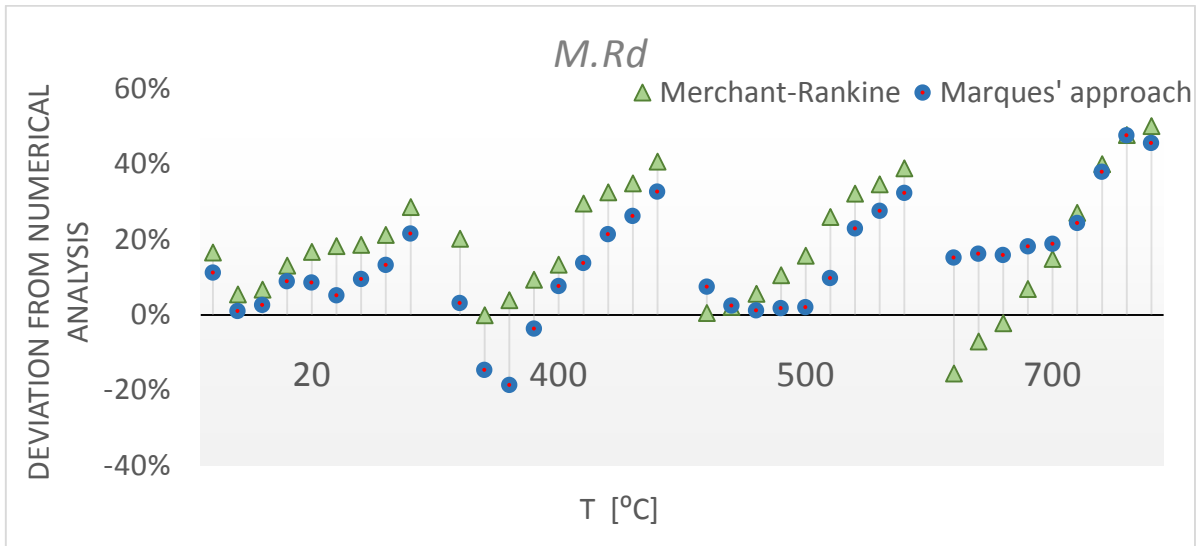
European Erasmus Mundus Master
Sustainable Constructions under natural hazards and catastrophic events
520121-1-2011-1-CZ-ERA MUNDUS-EMMC

surcos

20 °C

M.Rd

λ.bar.LT

	1.697	1.476	1.234	1.061	0.791	0.637	0.518	0.396	0.268
Marques' formulae	476.49	609.34	813.51	1002.00	1292.00	1284.00	1282.00	1278.00	1271.00
Abaqus	499.06	629.59	855.61	1108.58	1336.63	1311.30	1313.06	1324.10	1228.87
Merkant-Rankine	461.169	608.889	858.268	1093.395	1311.523	1327.713	1329.292	1329.465	1329.475
Eurocode	400.689	520.281	720.878	933.640	1329.475	1329.475	1329.475	1329.475	1329.475

Graph 4-20 Daviation of section resistance of beams T2, room temperature

400 °C

M.Rd

1.646 1.431 1.196 1.027 0.767 0.618 0.502 0.384 0.260

λ.bar.LT

500 °C

M.Rd

1.605 1.396 1.167 1.004 0.748 0.603 0.490 0.375 0.254
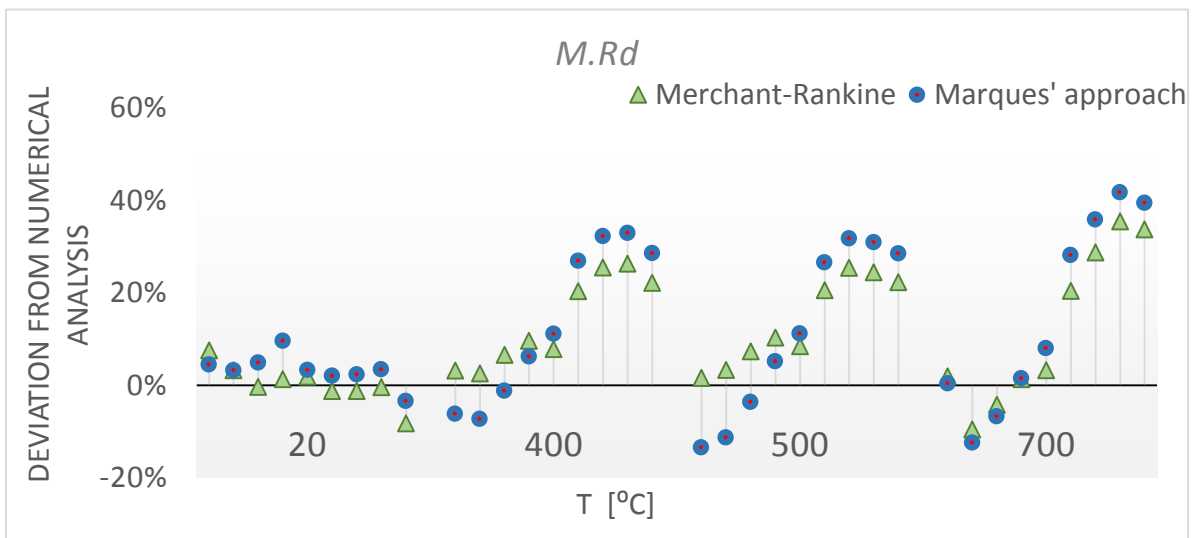
λ.bar.LT

Graphs 4-21 Daviation of section resistance of beams T2, various temperatures

Graph 4-22 Daviation of section resistance of beams T1, uniform load

Graph 4-23 Daviation of section resistance of beams T2, uniform load

The presented results show that even in the case of fire both procedures give relatively good results. Merchant-Rankin approach seems to be more suitable taking into consideration the simplicity of the application of this method. The problem here is that the results are highly dependent on the coefficient *n* which should be definitely studied more and checked on the very different types of tapered beams.

4.4 Final remarks

Tapered beams should be adopted in order to optimize the load capacity at each cross section according to the respective stress distribution. This is rising many questions up, such as what would be the cases in which the tapered member is worth applying, or, in which cases the effect of tapering is worth considering in the calculation.
- In case of uniformly distributed moments, definitely the prismatic beams should be adopted since in that way all cross sections would be fully utilized.
- For the triangular bending moment distribution, the higher the taper ratio the utilization of the cross section is more optimized.

The results obtained by numerical analysis are very well corresponding to the real behaviour of the beams. Still, finite element software usage requires some experience since the small differences in the model can lead to very different results.

When defining the relevant buckling modes to be accounted for in non-linear analysis, the deformation of the critical section (according to the first order utilization ration) is taken into account. Still, this is not always accurate. For example, when dealing with constant bending moment distribution on tapered member, the critical section that would be most logical to be chosen is the smallest section. This is valid assumption in the case of small taper ratios. But the bigger the taper is, the critical section is moving towards the middle of the member. The problem is that even the small change in the definition of the critical section influences results a lot since the cross section properties change rapidly in case of very tapered members.

Additionally, position of the critical section of one beam in elevated temperatures differs from the position defined in for the room temperatures for the same beam.

Also, it is hard to precise the position of critical section in GMNIA analysis since the resistance is sometimes reached by local buckling in the compressed flange or local (resp. shear) buckling of the web. This occurs in case of the very short beams (beam slenderness less than 0.5) and even though the results are not valuable in this study, they have been presented in the charts.

The results that were affected by shear were discarded since the analysis of the bending moment and shear interaction was not the topic of this research.

5 Conclusion

In this paper was studied lateral torsional stability of beams. Several ways of obtaining critical bending moment were compared. Also some existing approaches for the stability verification of web-tapered beams were analysed.

Even though there are many proposals for the elastic critical moment, all the solutions are complicated since many mistakes can be done when calculating. Some of them are calibrated just on particular loading cases. Based on the obtained results that are shown above, it can be seen that the existing tool (LTBeamN) for the definition of critical bending moment can be used. Besides from the accuracy of the results that it provides, this program is very easy to use and doesn't require powerful machine to run it. Also, LTBeamN has a possibility for taking into account the interaction between bending moment and axial force. Still, these cases were not investigated in this research.

As for the Marques' approach, it gives results which are mainly on the safe side. Somewhat better results are obtained by using imperfection factor $\alpha_p = 0.34$ and $\bar{\lambda}_{p0} = 0.8$ instead of the ones that are proposed for the class sections 1 and 2. These factors are the same ones that are proposed by Eurocode for the non-uniform beams of class 4. In case of elevated temperatures the results are not as accurate as in the case of room temperatures, but they are on the safe side. Here the over-strength factor is ignored (set to be equal to 1).

Merchant-Rankine approach gives satisfying results when using n coefficient equal to 1.5 in the case of elevated temperatures. In case of room temperatures results can be much improved when using this coefficient equal to γ_w.

Still, Eurocode approach gives pretty accurate results in case of beams of T1 which are of class 4. Taking into account the simplicity of the approach this might be the best approach in case of uniform bending moment distribution. On the other hand, when dealing with the beams at elevated temperatures, Eurocode gives unsafe results.

6 Acknowledgement

First of all, I would like to thank Ing. Michal Jandera Ph.D., the mentor and supervisor of this research. I am very grateful for his support, critics and valuable orientation for the development of this work. Secondly, I would like to thank the whole organization of SUSCOS Programme that gave me the opportunity to participate in it and for all the support they provided me. I would also like to thank the department colleague for all the help received during the research, namely Martin Prachař. Finally I would like to thank my family and friends that stood by my side during all the period.

7 References

[1]   Braham M, "Elastic lateral-torsional buckling of web tapered I-beams subjected to end moments", *Proceedings of the Slovak International Conference on Steel Structures and Bridges*, Brno, May 1997.

[2]   Boissonnade N, Braham M, "Elastic lateral-torsional buckling of tapered members with monosymmetric cross-sections: new approaches and correct solutions" (2002).

[3]   Marques L, Simões da Silva L, Greiner R, Rebelo C, Taras A, "Development of a consistent design procedure for lateral-torsional buckling of tapered beams" (May 2012).

[4]   Galéa Y. "Deversement des barres à section en I bissymétriques et hauter d´âme bilinéairement variable", Construction Métallique 23(2), pp. 50-54 (1986).

[5]   CEN, European Committee for Standardization, EN 1993-1-1:2005, *Eurocode 3: Design of steel Structures – Part 1-1: General Rules and Rules for Buildings*, Brussels, Belgium (2005).

[6]   Simões da Silva, L, Marques, L; Rebelo, C, "Numerical validation of the General Method in EC3-1-1 for prismatic members", Journal of Constructional Steel Research 66 (4), pp. 575-590 (2010).

[7]   Marques L, Simões da Silva L, Rebelo C, "Stability verification of web-tapered beam-columns – possible approaches and open questions" – *Proceedings of the Annual Stability Conference Structural Stability Research Council St. Louis, Missouri, April 16-20, 2013.*

[8]   Simões da Silva L, Simões R, Gervasio H, "Design of Steel Structures"*, ECCS Eurocode Design Manual (2010).*

[9]   CEN, European Committee for Standardization, EN 1993-1-2:2005, Eurocode 3: Design of steel structures - Part 1-2: General rules - Structural fire design, Brussels, Belgium (2005).

[10]   Simões da Silva L, Marques L, Rebelo C, "Application and validation of the interaction formulae in EC3-1-1 for stability verification of web-tapered beam-columns", ECCS Technical Committee 8, Paris, 2012

[11]   CEN, European Committee for Standardization, EN 1993-1-5:2006, Eurocode 3: Design of steel structures - Part 1-5: Plated structural elements, Brussels, Belgium (2005).

[12]   Marc Braham, Dominique Hanikenne, "Lateral Buckling of Web Tapered Beams: an original Design Method Confronted with a Computer Simulation" (1993).